Botanical Sciences 104 (1): 31-59. 2026
DOI: 10.17129/botsci.3738

Received: May 31, 2025, Accepted: October 5, 2025
On line first: November 26, 2025

Review / Revisión

Vegetation responses to paleoclimatic changes in Mexico: A review of palynological records

Manuel Zepeda-Pirron[1], Socorro Lozano-García[2, *], Margarita Caballero[3], Ken Oyama[4, 5]

[1] Posgrado en Ciencias de la Tierra, Instituto de Geología, Universidad Nacional Autónoma de México, Mexico City, Mexico.
[2] Instituto de Geología, Universidad Nacional Autónoma de México, Mexico City, Mexico.
[3] Instituto de Geofísica, Universidad Nacional Autónoma de México, Mexico City, Mexico.
[4] Escuela Nacional de Estudios Superiores Unidad Morelia, Universidad Nacional Autónoma de México, Morelia, Mexico.
[5] Laboratorio Nacional de Análisis y Síntesis Ecológica, ENES-Morelia, UNAM, Morelia, Mexico.
* Corresponding author: mslozano@unam.mx

Abstract
Climate is a key factor shaping plant communities. Given its high temporal variability, understanding the mechanisms behind community dynamics is essential. This review examines the role of climatic drivers such as the Intertropical Convergence Zone, North American Monsoon, Cold Fronts, El Niño-Southern Oscillation, and Atlantic Meridional Overturning Circulation, in both the present and the late Pleistocene and Holocene, using evidence from sedimentary proxies. We conducted a meta-analysis of palynological records from Mexico based on sedimentary sequences covering at least one glacial and one interglacial period. We focus on Marine Isotope Stages (MIS) 1 (14-7.2 kyr), 2 (29-14 kyr), 3 (57-29 kyr), 5e (126-116 kyr), and 6 (191-126 kyr) to assess how climate influenced plant communities. Results show clear contrasts between glacial and interglacial periods, except for MIS 2 and 3, highlighting region-specific responses to climatic forcing. Northern Mexico was strongly affected by the North American Monsoon, producing unexpectedly wetter conditions during MIS 2 than during the Holocene. In the Trans-Mexican Volcanic Belt, elevation plays a major role: the eastern mountains generate orographic rainfall and block moisture from reaching western areas, especially during glacial periods. In southern Mexico, vegetation shifts are linked to movements of the Intertropical Convergence Zone. These dynamics drive latitudinal and elevational vegetation migrations, and sometimes the emergence of non-analog communities. Understanding how long-term climate processes have historically shaped vegetation is crucial for informing conservation strategies in the context of ongoing global warming.
Keywords: Climate, paleoecology, pollen, meta-analysis, Quaternary.

Resumen
El clima constituye uno de los principales factores que determinan la composición y dinámica de las comunidades vegetales. Su alta variabilidad temporal hace imprescindible comprender los mecanismos que impulsan dichos cambios. En esta revisión se analiza el papel de distintos forzamientos climáticos como la Zona de Convergencia Intertropical, el Monzón de Norteamérica, los frentes fríos, El Niño-Oscilación del Sur y la Circulación Meridional de Vuelco del Atlántico, tanto en el presente como durante el Pleistoceno tardío y el Holoceno. Se presenta un meta-análisis de registros palinológicos en México, obtenidos de secuencias sedimentarias que abarcan al menos un periodo glaciar y uno interglaciar, con énfasis en intervalos específicos de los Estadios Isotópicos Marinos (MIS) 1 (14-7.2 ka), MIS 2 (29-14 ka), MIS 3 (57-29 ka), MIS 5e (126-116 ka) y MIS 6 (191-126 ka). Los resultados muestran contrastes claros entre periodos glaciares e interglaciares, con excepción del MIS 2 y 3, reflejando respuestas complejas y regionales a los forzamientos climáticos. En el norte, los sitios están fuertemente influenciados por el Monzón de Norteamérica, lo que ocasionó condiciones más húmedas durante el MIS 2 que en el Holoceno o el presente. En la Faja Volcánica Transmexicana, la vegetación respondió de manera diferenciada según la altitud, mientras que en el sur de México los cambios se vinculan a desplazamientos de la Zona de Convergencia Intertropical. Estos procesos propiciaron migraciones latitudinales o altitudinales de la vegetación y comunidades no análogas. Comprender estas dinámicas resulta esencial para diseñar estrategias de conservación ante escenarios climáticos futuros.
Palabras clave: Clima, paleoecología, polen, meta-análisis, Cuaternario.

Understanding climate dynamics is a priority for analyzing the physical, chemical, and biological processes that directly affect ecosystems. Mexico's climate is influenced by global and local dynamics. The interaction between Atlantic and Pacific Oceans, the country's location in the intertropical zone, and its topographical diversity result in a variety of climates and, consequently, diverse ecosystems, making it a region with high species richness and turnover. Lakes can preserve sedimentary sequences that serve as reservoirs of paleoclimatic and paleoecological information. Thus, the study of lacustrine sediments allows identification of climate changes and their effects on shaping communities (Schiferl *et al.* 2023). In particular, pollen studies enable the detection of changes in composition and structure of paleo-communities, many of them associated with climate variability, particularly during the Quaternary. However, pollen preservation in the records strongly depends on the characteristics and history of the study site, as desiccation processes in (paleo)lakes may destroy or render pollen grains unrecognizable, making their identification difficult (Lozano-García *et al.* 2002, Roy *et al.* 2013).

Palynological studies in Mexico date back to 1952, initially focusing on archaeological contexts (Sears 1952). Sears & Clisby (1955) conducted the first pollen analysis in lacustrine sediments in Mexico, identifying periods in which vegetation in the Basin of Mexico (BM) experienced significant compositional changes due to climate variations. Subsequent palynological studies on ancient sediments were conducted in different regions of the country (Hutchinson *et al.* 1956, Watts & Bradbury 1982, Straka & Ohngemach 1989). Although numerous palynological studies have been carried out in Mexico since then, only a few extend beyond the beginning of the Holocene (11,700 years Before Present [yr BP], hereafter 11.7 kyr). This date is crucial in geological and paleoclimatic terms as it marks a period of abrupt warming, the current interglacial, which was preceded by a glaciation period known as the Last Glacial Maximum (LGM) 22-18 kyr ago. Between LGM and the onset of the Holocene lies the deglaciation period. These periods exhibit significant global variations in precipitation and temperature, as evidenced by various physical, chemical, and biological signals, indicating that vegetation was not exempt from climate-driven changes.

In this review, we examine climate dynamics in Mexico and assess the effects of major climatic phenomena on plant communities. We first discuss the theoretical foundations of climate at a global scale and address the principal climatic drivers influencing Mexico. This study aims to identify changes in community composition in response to climate fluctuations across key regions of Mexico: (1) the Sonoran and Chihuahuan deserts and the northern part of the Sierra Madre Occidental; (2) the western zone of the Trans-Mexican Volcanic Belt (TMVB); (3) the eastern zone of the TMVB; (4) the southern region of the country. To achieve this, we conducted a meta-analysis of palynological records focusing on specific periods within Marine Isotope Stages (MIS) 1 (14 to 7.2 kyr), MIS 2 (29 to 14 kyr), MIS 3 (57 to 29 kyr), MIS 5e (126 to 116 kyr), MIS 6 (191 to 126 kyr) which correspond to episodes of significant climatic change. This approach enables the evaluation of vegetation responses across the sites and regions. Understanding vegetation responses to past climate variations provides a valuable framework for assessing future warming scenarios, anticipating their potential impacts on plant community composition and structure, and guiding conservation policies and forest management strategies.

(Paleo) Climatic Foundations

The primary driver of Earth's climate is solar energy. During the Quaternary, we can distinguish glacial (cold) and interglacial (warm) phases depending on the amount of energy reaching the earth surface at different latitudes. However, insolation is not the sole factor to consider, as climate results from the interaction of physical, chemical, and biological processes occurring within the planet's spheres: atmosphere, hydrosphere, geosphere and biosphere. The interactions and changes within these spheres drive climate variability across Earth's regions, influencing temperature, humidity, wind patterns, and precipitation through teleconnections.

A central element of climate dynamics in Mexico and the planet as a whole is the Hadley Cell, an atmospheric circulation system driven by surface temperature differences. This circulation involves the vertical movement of warm, moist air from the Intertropical Convergence Zone (ITCZ) near the equator toward higher latitudes, where it

descends in the subtropical region after losing moisture and energy. The Hadley Cell thus regulates the distribution of clouds and precipitation, and transport from low-to-mid latitudes of moisture (Cheng *et al.* 2022).

The following section will discuss the major climatic phenomena relevant to understanding Mexico's climatic configuration (Figure 1). In section 4 we relate and discuss the role of the major climatic drivers on vegetation changes over glacial and interglacial periods in Mexico.

Intertropical Convergence Zone (ITCZ). ITCZ is a low-pressure region where trade winds, laden with heat and moisture due to evaporation, converge. This creates a convective zone with high cloud cover and precipitation. ITCZ position varies depending on global temperature and ocean currents, leading to climatic phenomena both over the ocean and continents (Waliser & Jiang 2015, Figure 1).

ITCZ is closely linked to precipitation processes on Earth. It forms a band of convective clouds near the equator, extending approximately 6° in both hemispheres. However, its mean position is in the Northern Hemisphere due to greater landmass, which leads to higher warming. Seasonal migrations of ITCZ occur, shifting northward in boreal summer and southward in winter (Samuel *et al.* 2023). In the Atlantic and Pacific Oceans, its mean summer position in the Northern Hemisphere is around 9° N, while in winter, it shifts to 2° N. On paleoclimatic scales, a similar pattern has been reconstructed: during warm years, ITCZ migrates northward, whereas in colder years, it moves southward, except during El Niño years (Schneider *et al.* 2014).

Both climate models and paleo-reconstructions based on proxy data indicate that ITCZ migration responds to hemispheric temperature contrasts. Reduced precipitation in Central America is linked to southward ITCZ displacement over the Pacific, associated with Southern Hemisphere warming and Northern Hemisphere cooling, particularly in the eastern Pacific. Sediment records from the Cariaco Basin, based on Ti and Fe concentrations, also support temperature-driven ITCZ shifts, with northward movement during warm periods such as the Holocene Thermal Maximum (~6 kyr), and southward during cold intervals like the LGM (Haug *et al.* 2001, Zhang & Delworth 2005, Chiang & Friedman 2012). Yuan *et al.* (2023) highlight discrepancies between computational models and proxy-based studies regarding the climatic effects on ITCZ migration: while models indicate minimal latitudinal shifts, proxies reveal significant gradients. However, interpreting paleo-records remains complex due to interactions with broader atmospheric circulations. Modern observations under La Niña/El Niño conditions show significant variability in ITCZ position, strength, and amplitude. Yuan *et al.* (2023) also document intensification of the ITCZ from the LGM to the Holocene, marked by a low-amplitude, southern-positioned ITCZ during glacial periods, and a northward-expanded system after the Holocene onset.

Satellite data and simulations indicate that both ITCZ amplitude - the distance between the northern and southern boundaries of the Hadley Cells - and its intensity are expected to decrease due to global warming (Byrne *et al.* 2018) suggesting ITCZ structure has a nonlinear relationship with temperature.

ITCZ migration is influenced by both interhemispheric temperature contrasts and oceanic heat transport. Regarding temperature contrast, Broccoli *et al.* (2006) developed a climate model showing Northern Hemisphere cooling and Southern Hemisphere warming, where ITCZ migrates southward. Their study shows that heat exchange in tropical-midlatitude drive ITCZ variability.

North American Monsoon (NAM). NAM, also known as the Mexican Monsoon, is a climatic circulation that represents a significant proportion of precipitation across most of Mexico and southern U.S. (Metcalfe *et al.* 2015). NAM has three branches: one in the Pacific and two in Gulf of Mexico. Atlantic branches are part of the Caribbean Low-Level Jet (CLLJ), discussed in section 2.2.1 (Figure 1). During boreal summer, land heats up more rapidly than Gulf waters, creating a low-pressure zone over northern Mexico and southern U.S. This pressure gradient facilitates the transport of warm, humid air from the Caribbean and the Gulf via CLLJ, resulting in orographic rainfall (Boos & Pascale 2021).

The Pacific branch is the most studied, especially in the "core region" of NAM: New Mexico and the southwestern U.S. (Metcalfe *et al.* 2015). During boreal summer surface air temperature decreases in eastern Pacific, leading to the formation of an anticyclone (a high-pressure center emitting winds) in the upper troposphere, which transports moisture from ITCZ toward the Sierra Madre Occidental and the southwestern U.S. (Routson *et al.* 2022). Although

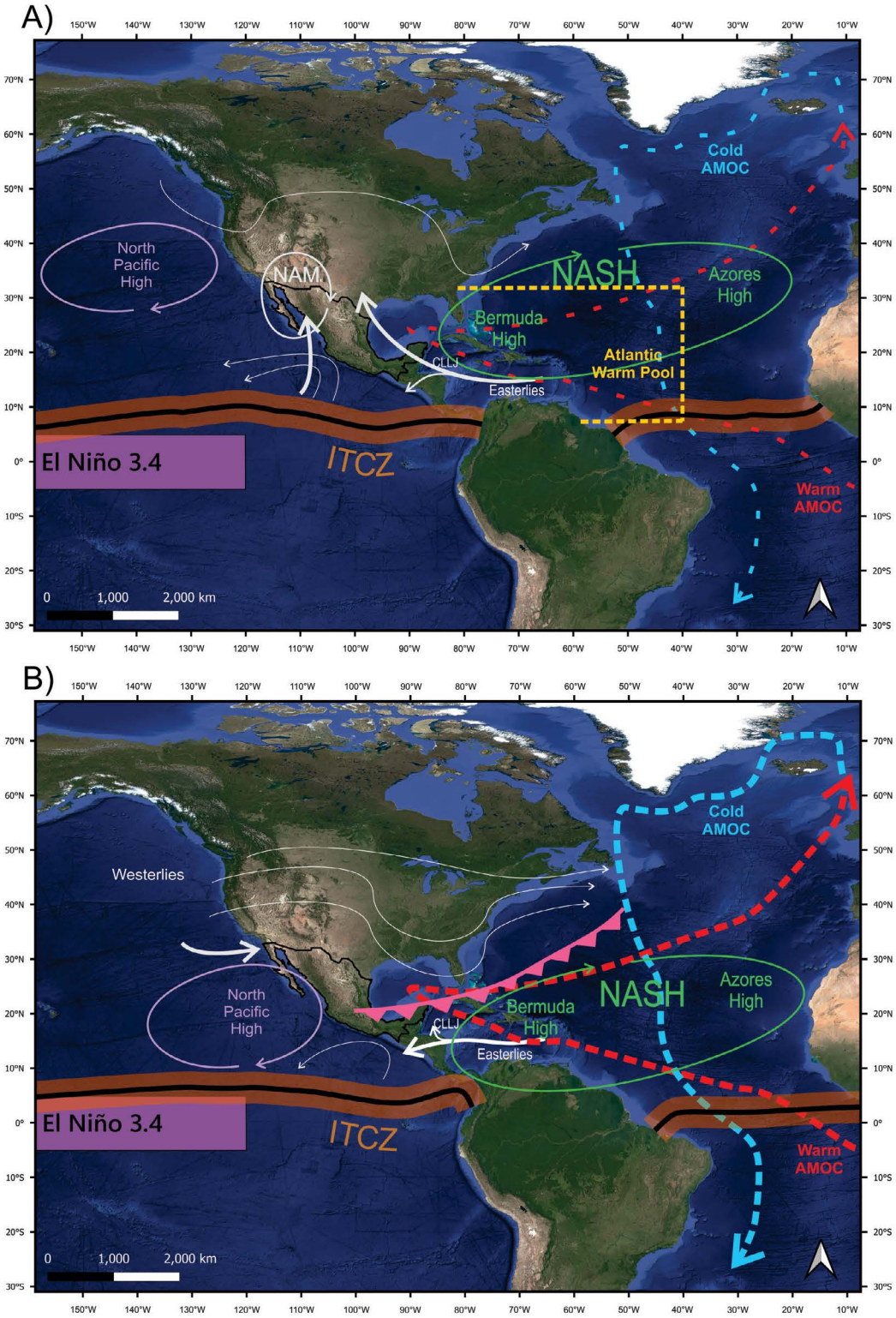

Figure 1. Climate model for North America. A) Summer and Interglacial. B) Winter and Glacial. Modified from Metcalfe *et al*. 2015 and based on Chen et al. 2019, Lyle *et al*. (2010), Luo *et al*. (2021), Muñoz *et al.* (2008), Ritz *et al*. (2013), Samuel *et al*. (2023), Wang & Lee (2007). Intertropical Convergence Zone (ITCZ); Atlantic Meridional Overturning Circulation (AMOC); Caribbean Low-Level Jet (CLLJ); North Atlantic Subtropical High (NASH); North American Monsoon (NAM).

evaporation from the Gulf of California and the Pacific Ocean is the primary source of moisture in the Pacific branch of NAM, evapotranspiration from the Sierra Madre Occidental also plays an important role, suggesting that NAM is broader and more complex than just its core region (Bhattacharya *et al.* 2018).

The Bermuda High (BH), an extension of the North Atlantic Subtropical High (NASH), plays a crucial role in NAM seasonality. During summer, it migrates northward, promoting the flow of warm, moist easterlies across Mexico and Central America. Orographic barriers like the Sierra Madre Oriental limit moisture transport to the southwestern U.S., although some reaches the Great Plains (Metcalfe *et al.* 2015). Luo *et al.* (2021) add that the BH also shifts east-west interannually: eastward displacement increases rainfall in the southeastern U.S. and central-eastern Mexico, while westward shifts reduce it.

In the Pacific, increasing Sea Surface Temperature (SST) allows stratified air - warm and humid near the surface, dry and cooler above - to mix and travel across the Gulf of California, forming intense storms in NAM core region. As warmer SST moves closer to the coast, monsoonal convection shifts northward (Erfani & Mitchell 2014). Both rising SST and strong seasonality during summer in the Gulf of California promote monsoonal convection (Routson *et al.* 2022). Unlike the Sierra Madre Oriental, the Sierra Madre Occidental acts as a conduit for warm, moist winds traveling through the Gulf of California (Metcalfe *et al.* 2015).

Westerlies influence NAM by modulating atmospheric ventilation. When moist Atlantic and Pacific airflows dominate, weak ventilation occurs: westerlies are displaced, allowing anticyclones to migrate northward and enhancing convection. In contrast, strong or southward-shifted westerlies inhibit monsoonal activity (Routson *et al.* 2022). Metcalfe *et al.* (2015) link this to seasonal patterns—westerlies weaken in summer and intensify in winter (Figure 1). Their strength reflects the temperature gradient between the equator and the Arctic, which decreases under planetary warming as high latitudes warm more rapidly than the tropics (Routson *et al.* 2019).

During past warming periods, such as the mid-Holocene, a weakened temperature gradient coincided with significantly reduced precipitation at mid-latitudes, indicating that weaker gradients reduce westerlies and mid-latitude precipitation (Routson *et al.* 2019). This suggests similarities between glacial and winter conditions, as well as between interglacial and summer conditions.

Caribbean Low-Level Jet (CLLJ). Low-Level Jets (LLJs) are fast-moving winds in the lower troposphere relative to their surrounding region. The Caribbean LLJ, driven by Easterly Winds, are part of the Hadley Cell and originate in the Atlantic, making it an extension of BH and NASH (Muñoz *et al.* 2008).

During the boreal summer, ITCZ migrates northward, favoring subtropical precipitation. However, this pattern is absent in the Caribbean. One explanation involves low-level wind jets, ocean-land contrasts, orography and convection (Muñoz *et al.* 2008). This anticyclonic zone transports significant moisture from the Caribbean to Central America, the Gulf of Mexico, and the southern U.S., contributing to the North American Monsoon system (Maldonado *et al.* 2017). The maximum intensity of the Easterly Winds follows a semi-annual pattern, peaks in summer and winter, with minima in spring and autumn (Wang 2007).

The intensity of the Easterly Winds opposes convection in CLLJ region (Maldonado *et al.* 2017). Wang (2007) suggests that strong easterlies and high sea-level pressure (SLP) in July, result in reduced precipitation and fewer tropical cyclones in the Caribbean. This phenomenon, the Mid-Summer Drought or *Canícula* was first explained by Magaña *et al.* (1999). Conversely, in October, when SSTs peak in the region, precipitation and tropical cyclone activity also increase. Thus, strong Easterly Winds enhance moisture transport from the Caribbean toward North and Central America, reducing convection over CLLJ region. Muñoz *et al.* (2008) further explain that pressure differences in the region are partially influenced by the high mountains along the Caribbean's boundary, creating significant temperature contrasts between the ocean and the continent.

The variability of the Caribbean LowLevel Jet (CLLJ) is driven by seasonal SST and sealevel pressure (SLP) gradients, along with its internal vertical structure and frictional processes. SST and SLP gradients exhibit semiannual coupling aligned with CLLJ variation, linked to migration of the NASH across seasons: NASH remains in the western Atlantic during summer and winter, shifting eastward in spring and autumn. Simulations suggest mountain

height and SST gradients are secondary drivers. Instead, barotropic atmospheric instability—due to horizontal and vertical wind shear—and interactions between the CLLJ's vertical profile and surface-layer friction dominate its dynamics (Wang 2007, Maldonado *et al.* 2017).

Although the structure of CLLJ remains debated, studies have shown its teleconnections with El Niño Southern Oscillation (ENSO). Wang (2007) identified a relationship between Pacific SSTs and CLLJ variability, suggesting that SST-CLLJ interactions depend on seasonal SLP anomalies: negative in winter, positive in summer. During winter, weak Easterly Winds associated with CLLJ correspond to warm SST anomalies in the eastern Pacific, and vice versa. In summer, strong Easterly Winds correlate with warm anomalies in the Pacific. García-Martínez & Bollasina (2020) developed models linking increased drought periods in southeastern Mexico to intensified CLLJ activity. In contrast, they observed increasing rainfall in the eastern Pacific. This teleconnection is associated with high- and low-pressure cells at different atmospheric levels.

Few paleoclimatic reconstructions of past CLLJ exist, but Studholme *et al.* (2022) suggest that following the precession minimum at MIS 2-MIS 1 transition, increased insolation amplified tropical convection and strengthened mid-latitude jets, placing tropical cyclones near current positions. Conversely, during cold events such as Heinrich events, a weakened AMOC altered the Northern Hemisphere's meridional temperature gradient, intensifying both the Subtropical Jet and the Hadley Cell while shifting them toward the equator. This displacement caused tropical cyclones to migrate southward (Studholme *et al.* 2022).

Lozano-García *et al.* (2015) reported lower precipitation in BM during LGM compared to the deglaciation period, in contrast to sediment core studies near the southern Gulf of Mexico. Their findings suggest that the north-south migration of ITCZ alone does not explain these variations. Instead, they propose that reduced AMOC during the glacial period expanded the Atlantic Warm Pool (AWP) in the Gulf of Mexico during summer due to stagnant water movement, leading to increased precipitation in southern regions. AWP is a region of warm ocean water extending across the Gulf of Mexico, the Caribbean, and parts of the western Atlantic between summer and autumn, defined by SST above 28.5 °C (Wang & Lee 2007, Figure 1). During the Holocene, the AWP reached its maximum extent and persisted for most of the year, causing dry conditions in central/southern Mexico and wetter regions due to CLLJ.

Cold fronts or "Nortes". Cold fronts result from the collision between a cold and a warm air mass. Differences in temperature, density, and humidity cause atmospheric instability. Cold air masses form at high latitudes via polar circulation, near the northern edge of the Hadley Cell. Since cold air is denser, it moves beneath the warm air, forcing the latter to rise. As the warm air ascends, it cools adiabatically, condensing moisture and producing rainfall (Metcalfe *et al.* 2000).

Cold fronts in North America are common during the boreal winter because ITCZ shifts southward, and warm air no longer blocks cold air from reaching the Sierra Madre Oriental and Gulf of Mexico (Passalacqua *et al.* 2016). In contrast, during the boreal summer, the Hadley Cell constrains polar air currents (Piacsek *et al.* 2024, Figure 1).

Paleoenvironmental studies provide evidence of changes in the frequency of *Nortes* (cold surges). For instance, by analyzing stable isotopes and trace elements in speleothems, Piacsek *et al.* (2024) found that during the Little Ice Age (1400-1850 CE), trade winds linked to NASH were weaker. This condition favored the North Atlantic Oscillation (NAO) remaining negative: the pressure gradient between the Azores High and the Icelandic Low was reduced. As a result, winters in North America were colder, and frontal rainfall increased.

El Niño-Southern Oscillation (ENSO). ENSO is an unstable oceanic-atmospheric pattern in the tropical Pacific, causing major interannual climatic variability (Emile-Geay *et al.* 2016). ENSO reflects the coupling between oceanic dynamics and atmospheric response to SST changes (Tian *et al.* 2017). The warm SST phase is known as El Niño, while the cold phase is called La Niña. The Southern Oscillation is the atmospheric component that co-varies with SST.

ENSO is best understood by first describing normal Pacific conditions. Strong trade winds move from east to west across the Pacific via the Walker Circulation, steepening the thermocline (warm water at the surface and cold water at depth). This steep thermocline enables eastern Pacific upwelling, as warm water accumulates in the west, generating

convection and precipitation (Chen *et al.* 2019). El Niño is monitored using the Niño 3.4 index (5° N - 5° S, 120° W - 170° W, Figure 1), where variations in precipitation, temperature and productivity are significant between the different phases.

Both El Niño and La Niña are destabilizations of normal climatic conditions due to positive feedback mechanisms within these cycles. For example, in El Niño the weakening of trade winds results in a reduction of the thermocline slope, leading to a greater accumulation of warm water in the eastern Pacific. In turn, this warming further weakens the trade winds and disrupts Walker Circulation, reinforcing El Niño conditions. In contrast, during La Niña conditions, an increase in trade wind strength amplifies the thermocline slope, accelerating the east-to-west transport of warm water across the Pacific, making Walker Circulation more intense (Chen *et al.* 2019). Despite the positive feedback process, ENSO variability can be interrupted by thermocline adjustments, though the mechanisms behind this remain unclear due to ENSO's complexity and its influence across different timescales, including annual, decadal, and multi-decadal scales (Stuecker 2018, Chen *et al.* 2019).

ENSO significantly affects Mexico: during El Niño years, northern regions receive winter rains, while La Niña brings droughts (Brunelle *et al.* 2024). ENSO also plays a key role in the formation of tropical cyclones in both oceans due to its influence on wind shear intensity (Maloney & Hartmann 2000). During El Niño years, the probability of hurricanes forming in the Atlantic decreases, while during La Niña years, the likelihood increases. While many studies focus on ENSO's short-term effects under global warming, fewer studies have reconstructed its past variability. Koutavas & Joanides (2012) analyzed isotopes in planktonic foraminifera, finding that ENSO was more intense during cold periods like LGM or Younger-Dryas due to a weaker temperature gradient in the eastern Pacific. In contrast, during the mid-Holocene and other warm periods, ENSO weakened due to a stronger thermal gradient. They propose that precession forcing is a major driver of ENSO intensity. Also, through the analysis of planktonic foraminifera, Stott *et al.* (2002) found that during glacial periods, SST resemble El Niño events, with southward ITCZ shifts and weakened Walker circulation. In interglacials, conditions resembled La Niña. Other studies suggest that ENSO intensity during the Holocene has been highly dynamic. Emile-Geay *et al.* (2016) reconstructed Pacific conditions using mollusks and corals, concluding that ENSO and orbital forcing lack a linear relationship, suggesting internal processes may dominate.

Atlantic Meridional Overturning Circulation (AMOC). AMOC is an oceanic flow that distributes heat latitudinally through a cycle. Warm, salty surface water flows to the North Atlantic from the tropics. Along the way, the water loses energy and moisture to the atmosphere. As a result, the water cools, become saltier and sinks in the North Atlantic to form the North Atlantic Deep Water (NADW). The deep water then flows southward and resurfaces in the South Atlantic, completing the cycle (Ritz *et al.* 2013, Wang *et al.* 2023, Figure 1). Dansgaard-Oeschger (D-O) events, marked by abrupt warming and gradual cooling in the North Pole, are linked to AMOC variability and has been recorded mainly in Greenland ice cores (Ritz *et al.* 2013). Although their origin is not fully understood, models suggest that Southern Hemisphere temperatures during glacials can trigger abrupt AMOC shifts once a threshold is crossed (Oka *et al.* 2021). Heinrich events, caused by iceberg discharges into the North Atlantic, add freshwater that disrupts ocean density and weakens AMOC circulation, thereby reducing energy transport (Lynch-Stieglitz *et al.* 2014).

On millennial scales, AMOC weakening is associated with Northern Hemisphere cooling and Antarctic warming (Buizert *et al.* 2015, Henry *et al.* 2016). Antarctic warming phases often end abruptly after Greenland temperature rises, especially during strong D-O events (Oka *et al.* 2021). Heinrich 1 and the Younger Dryas show significant AMOC weakening (Ritz *et al.* 2013, Lynch-Stieglitz *et al.* 2014), while Heinrich 2 and 3 show less change, possibly due to preexisting weakening caused by ocean stratification during glacial periods. Thus, weakening during Younger Dryas and Heinrich 1, 4, and 5 reflects shifts from weak (warm) to strong (cold) stratification by glacial meltwater forcing (Lynch-Stieglitz *et al.* 2014). Henry *et al.* (2016) suggests that during MIS 3, AMOC weakened during Northern Hemisphere cooling, especially during Heinrich events, but recovered with subsequent warming (Figure 2).

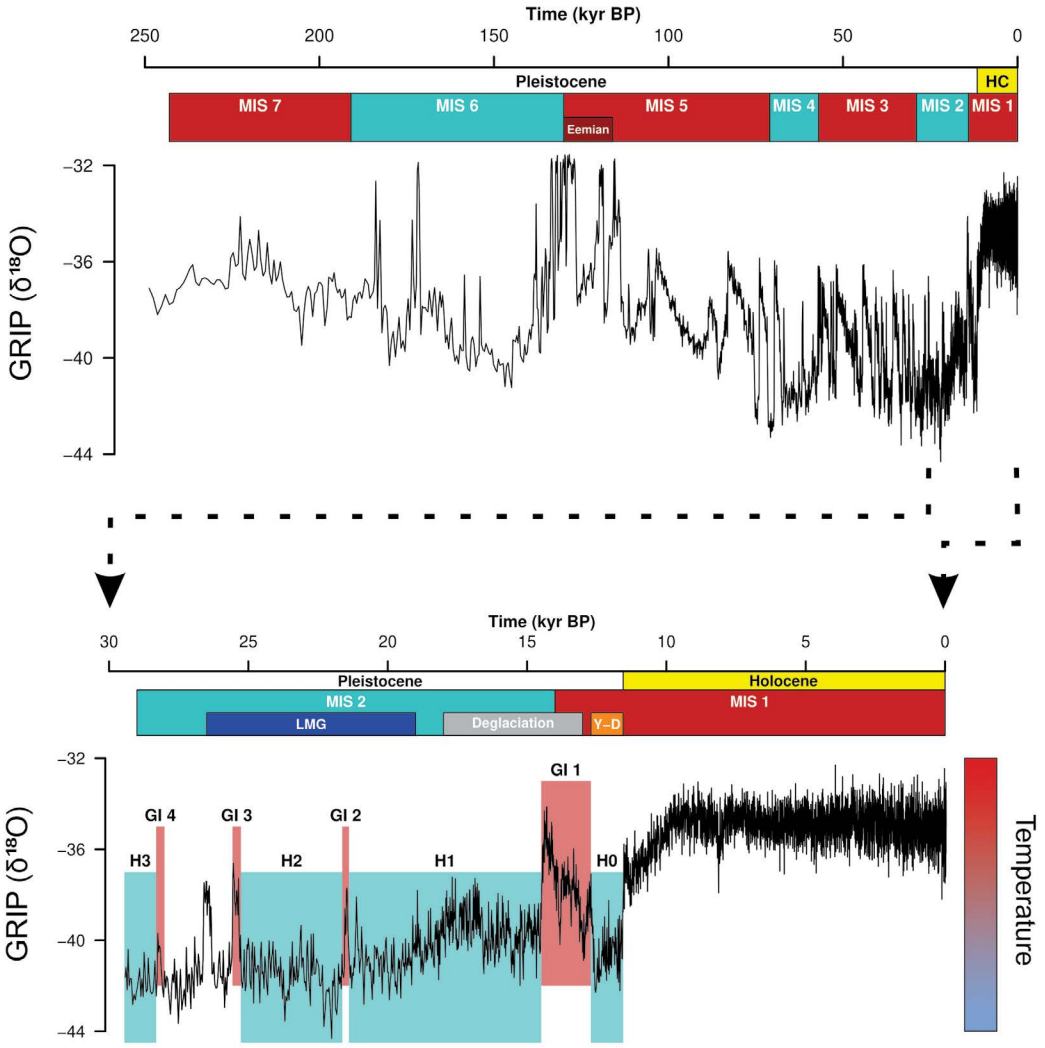

Figure 2. $\delta^{18}O$ in GRIP core from the last 250 kyr (Dansgaard et al. 1993). MIS boundaries defined by Lisiecki & Raymo (2005). Heinrich and Greenland Interstadial events defined by Björck et al. (1998). Marine Isotope Stage (MIS); Last Maximum Glacial (LMG); Deglaciation (Dg); Younger Dryas (YD); Holocene (HC); Heinrich event (H), Greenland Interstadial (GI), also known as D-O events.

Recent paleoclimatic multiproxy studies continue to identify the same pattern: AMOC underwent significant changes during the last Glacial-Interglacial cycle, coinciding with Heinrich events (Liu 2023). Furthermore, the effects of Heinrich and D-O events on the climate of BM have been reconstructed. Caballero *et al.* (2019) analyzed diatom-based temperature and precipitation reconstructions from Lake Chalco, showing D-O events were humid, while Heinrich events were dry. Meltwater from glaciers entering the North Atlantic causes a thermal shock that weakens AMOC and reduces heat transport to the tropics. Consequently, ITCZ migrates southward, decreasing monsoon activity in the Northern Hemisphere (Caballero *et al.* 2019).

As AMOC-driven heat transport variations may influence ITCZ positioning, both cooling and increased ice cover in the North Atlantic also contribute to ITCZ modifications, implying AMOC is not the sole driver of these climatic shifts (Lynch-Stieglitz *et al.* 2014). Tropical-high latitude climate links depend on ITCZ position shifts, as warm (cold) events in Greenland correspond to a more northern (southern) ITCZ position. Studies show AMOC is vulnerable to warming scenarios. This may either reduce its capacity to transport warm water northward or halt circulation entirely. As a result, a "warming hole" has been observed in the North Atlantic (Keil *et al.* 2020). More-

over, meltwater from Greenland could rapidly cool the North Atlantic enough to shut down AMOC, triggering a new D-O event (Broecker *et al.* 1985).

Materials and methods

One of the major challenges in paleoclimatology is integrating climate responses from palynological records obtained at different sites. Metcalfe *et al.* (2000) carried out a review of paleo-reconstruction studies in Mexico using different proxies; the present review updates the palynological analysis that proposes a quantitative synthesis providing insight into vegetation responses to broad climatic trends. To address this issue, we conducted a meta-analysis of the literature published up to 2024. The keywords *Pollen*, *Paleoclimate*, and *Mexico* were searched in both Scopus and TESIUNAM.

The inclusion criteria consisted of peer-reviewed articles or theses from UNAM that focused on paleoenvironmental reconstructions based on palynological analyses, in which it was possible to retrieve measurements from at least one interglacial and one glacial period. Studies that did not meet these requirements or that did not provide databases accessible through repositories such as Neotoma (apps.neotomadb.org) or UNAM's Open Data Portal (datosabiertos.unam.mx) were excluded from the meta-analysis, although they were included in the Discussion section. In some cases, information had to be extracted from digitized data (see S1). Some studies were not considered in this review due to their age models inconsistencies.

We conducted a regionalization of these studies, as nearby sites show similar signals over the same periods, while significant variations exist between regions due to Mexico's diverse climatic conditions. For each region, we described the general climatic conditions and associated vegetation (S2). Additionally, we analyzed vegetation composition changes based on pollen assemblages from sedimentary records during glacial-interglacial transitions to identify the climatic patterns underlying vegetation shifts, such as altitudinal or latitudinal migrations.

For the meta-analysis, 16 palynological sequences were used (Figure 3). The response variable considered in this review was the percentage of arboreal pollen, for which the mean, standard deviation, and the number of samples corresponding to each MIS were obtained. Calibrated ages from the age-depth models reported in each study were used to assign samples to MIS 1, MIS 2, MIS 3, MIS 5e, or MIS 6 (Lisiecki & Raymo 2005, Salonen *et al.* 2018). For studies that did not provide calibrate ages, new age-depth models were developed from the reported uncalibrated radiocarbon dates (S1) using the R (R Core Team 2024) package Bchron (Haslett & Parnell 2008) with calibration curve IntCal20.

The explanatory variables used to assess data variability were the study region, the corresponding MIS, elevation, elevational range (*i.e.*, the difference between the elevation of the lacustrine record and that of the surrounding highest point), and the interaction between the last two variables. In this context, we assumed that the effect of elevation on the analyzed variables depends on the elevational range, and vice versa. A random effect was fitted by site, and the restricted maximum likelihood (REML) method was applied. The significance of the comparisons between the different levels of the factor across the MIS and the regions was adjusted using Hommel's method (1988), which is useful for controlling the familywise error rate and preventing Type I errors due to multiple comparisons. Analyses were conducted in R (R Core Team 2024) using the package metafor (Viechtbauer 2010).

Pollen records

Sonoran Desert.

1) Ciénega Chimeneas (1,335 m asl). Brunelle *et al.* (2024) obtained a sedimentary sequence which spans from 44 to 9.5 kyr (Figure 3). Annual precipitation in this region is approximately 600 mm, with more than half occurring in winter due to cold fronts. During El Niño events, precipitation tends to increase. Vegetation includes xerophytic scrub and oak forests in the lowlands, with pine-oak forests at higher elevations. The oldest part of the record (40 kyr, MIS 3) shows dominance of taxa linked to summer rainfall, such as *Ambrosia*, *Larrea*, *Quercus*, Asteraceae, and Amaranthaceae. *Artemisia*, associated with winter precipitation, was present but less abundant. At the onset of MIS

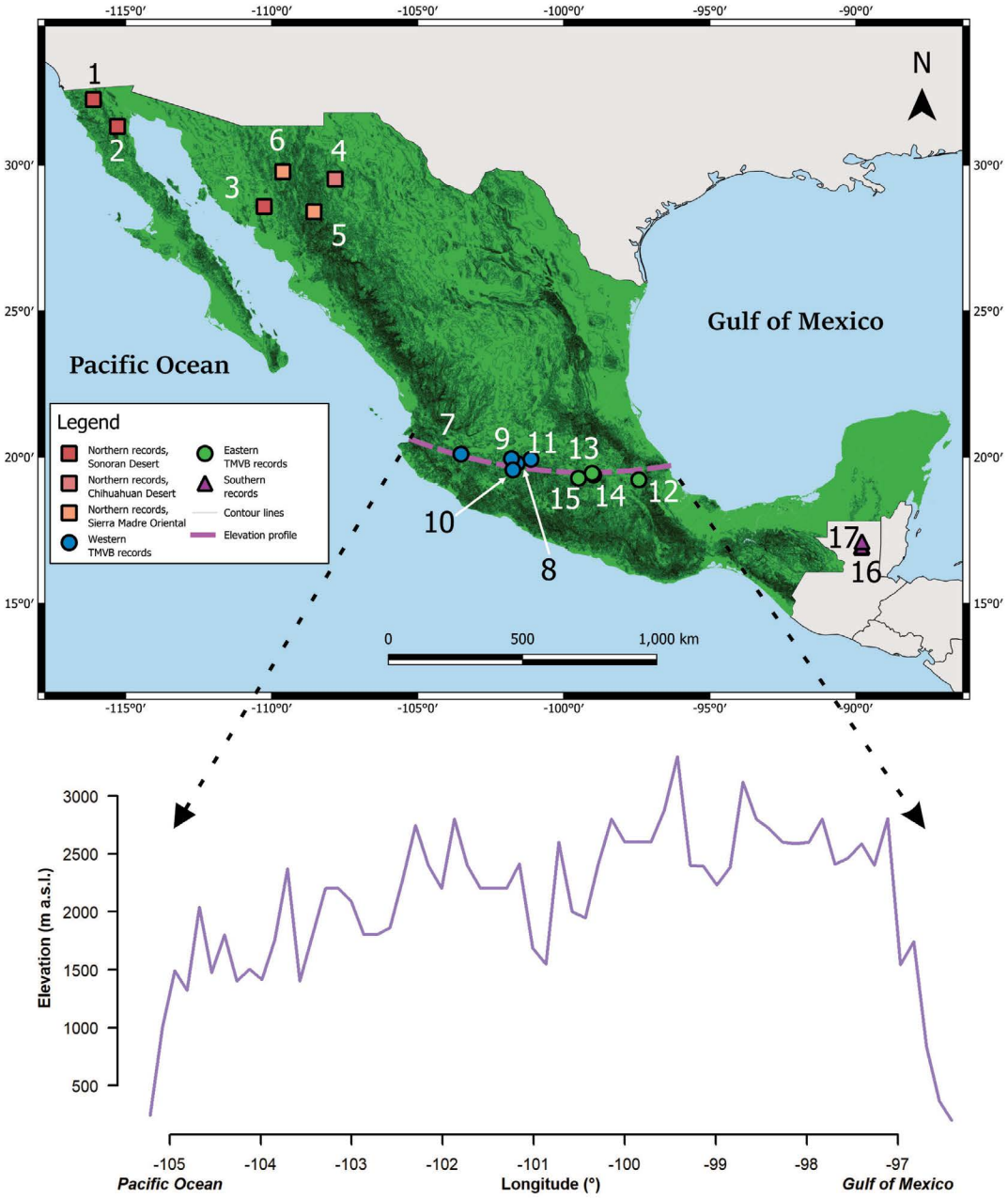

Figure 3. Pollen records in Mexico. Squares represent the sedimentary sequences with palynological data from the Northern region, circles the Central (blue-West, green-East) region and triangles the Southern region. Dotted line shows the elevational profile (m asl) from West to East of Transmexican Volcanic Belt. Numbers show sedimentary cores with pollen analysis (Table S1).

2, *Ambrosia* and Amaranthaceae declined, while *Artemisia*, Asteraceae, and Poaceae increased. During the LGM and deglaciation (21-14 kyr), *Ambrosia*, Asteraceae, Amaranthaceae, Brassicaceae, and Rhamnaceae were prominent. *Larrea* and *Quercus* reappeared only in the Holocene. The mixture of summer- and winter-adapted taxa during the LGM suggests a shift in precipitation patterns. In the Late Glacial-Holocene transition (14-10 kyr), increased abundance of *Larrea*, *Quercus*, *Artemisia*, *Pinus*, Poaceae, and Cyperaceae points to higher annual rainfall, likely from enhanced winter precipitation (Table 1).

2) San Felipe (400 m asl). Lozano-García *et al.* (2002) reported a pollen record from a lacustrine sequence spanning from 44 to 13 kyr (Figure 3). Today, it is part of the regions in North America with the lowest precipitation and highest insolation. The vegetation in lowland areas consists of microphyllous desert plants. In the mountainous areas (Sierra de San Felipe), humidity is higher than in the lowlands, allowing the presence of open forests. At ~40 kyr, vegetation showed high herbaceous richness, including *Allonia incarnata*, *Plantago*, *Rubiaceae*, *Artemisia*, Amaranthaceae, and Asteraceae. Arboreal taxa included *Pinus*, *Juniperus*, and *Quercus*, with *Abies* appearing intermittently. Around 30 kyr (onset of MIS 2), vegetation was dominated by alternating *Pinus* and *Juniperus*, with less common *Arctostaphylos* and *Quercus*. Amaranthaceae, *Artemisia*, and *Ambrosia*, typical of high elevations in the Sierra de San Felipe, were also present. During the LGM (~22 kyr), *Pinus* increased while *Juniperus* declined, indicating downward migration due to wetter conditions. In the deglaciation (~18-13 kyr), *Juniperus* expanded as *Pinus* and herbaceous taxa declined. After 13 kyr, pollen was no longer preserved due to complete lake desiccation driven by rising Holocene temperatures (Table 1).

Table 1. Summary of the pollen records from the northern region for MIS 1, MIS 2, MIS 3 and associated climate drivers of vegetation changes. Site number correspond to those indicated in the sedimentary records section. ">" is used for "increase, "<" for decrease, T° for temperature, Pp for precipitation and NR refers to no record.

Site	Current vegetation (low-high altitudinal gradient)	MIS 1 (14 - 7.2 kyr) Pollen / Driver	MIS 2 (29 - 14 kyr) Pollen / Driver	MIS 3 (57 - 29 kyr) Pollen / Dirver
1	Shrubs, sage-chaparral-oak woodland, pine-oak forest	> *Larrea* and *Quercus* / > Winter Pp, El Niño conditions	< *Ambrosia* and Amaranthaceae, > *Artemisia*, Asteraceae and Poaceae / > Summer Pp, La Niña conditions	> *Ambrosia*, *Larrea*, *Quercus*, Asteraceae, Amaranthaceae / > Winter Pp, El Niño conditions
2	Sparse microphyllus scrubs, open woodlands, coniferous forest	**NR** / Lake desiccation. < Pp, strong NAM	> *Pinus*, *Artemisia*, *Ambrosia* < *Juniperus* / > Pp, weak NAM	> *Allonia incarnata*, *Plantago*, Rubiaceae, *Pinus*, *Juniperus*, *Quercus* / Strong NAM
3	Desert scrub, tropical deciduous forest, pine-oak forest	**>** *Bursera*, *Parkinsonia*, Asteraceae, Fabaceae < *Pinus*, *Juniperus* / < Pp, strong NAM	> *Juniperus*, *Pinus*, *Quercus* / > Pp, weak NAM	**NR**
4	Halophytic grassland, pine-oak forest	**NR** / > Summer Pp, strong NAM	> *Pinus* and *Picea* < *Quercus,* shrubs and grasses / > Winter Pp, weak NAM	> *Quercus* and Poaceae / > Summer Pp, strong NAM
5	Grassland, pine-oak forest	> *Quercus, Poaceae* < *Abies, Pinus* / > T° < Pp, strong NAM	**NR**	**NR**
6	Thorn scrub and grassland, pine-oak forest	> Amaranthaceae, Ambrossinae, Poaceae < *Pinus* / < Pp, strong NAM	> *Pinus, Abies, Picea* < Amaranthaceae, Ambrosiinae, Poaceae / > Pp, weak NAM	**NR**

3) Ciénega San Marcial (335 m asl). Ortega-Rosas *et al.* (2016) conducted a paleoenvironmental reconstruction based on pollen records from the Ciénega San Marcial, a site strongly influenced by NAM. The sedimentary sequence spans from 15.6 kyr, but due to the nature of the cienega, a hiatus exists between 13.4 kyr and 1919 Common Era (CE). This allows for analysis of vegetation dynamics during the end of the glacial. Present-day vegetation varies by elevation: desert scrub in lowlands, tropical deciduous forest at mid elevations, and pine-oak forests at higher elevations (S2). The climate is desert-like, with an average annual temperature around 23 °C and precipitation ranging from 250 to 350 mm/year, most of which occurs during the summer. Around 15.5 ka, forests dominated by *Juniperus*, *Pinus*, and *Quercus* were abundant, while herbaceous taxa such as *Artemisia*, *Ambrosia*, Asteraceae, and Poaceae were less frequent. Estimated temperatures were about 10 °C cooler than today, with annual precipitation around 550 mm, mostly falling in winter. Toward the end of MIS 2 (15-13 kyr), arboreal taxa like *Pinus* and *Juniperus* declined, as *Bursera*, *Parkinsonia*, Asteraceae, and Fabaceae became more common, suggesting temperatures were about 5 °C lower than present, with annual rainfall reaching approximately 600 mm.

Chihuahuan Desert.

4) Alta Babícora (2,138 m asl). Metcalfe *et al.* (2002) recovered a sedimentary sequence dating back to 65 kyr. This basin, located in the northern Sierra Madre Occidental, reaches elevations up to 3,000 m asl. Annual precipitation varies between 500 and 1,000 mm depending on the area, with most rainfall occurring in summer (July-October). The present-day vegetation is divided into two communities: pine-oak forest and halophytic grassland (Estrada *et al.* 1997). During MIS 3, *Quercus* and Poaceae were abundant, with lesser amounts of *Picea* and *Pinus*. Toward the MIS 3-2 transition, *Juniperus* increased while *Ambrosia* declined. In MIS 2, a major shift occurred: *Pinus* and *Picea* dominated, while *Quercus*, shrubs, and grasses (including pasture species) nearly disappeared, indicating cooler and wetter conditions than today. Notably, *Picea* is now nearly extinct in the Sierra Madre Occidental. At the beginning of the Holocene, pollen preservation was poor, limiting identification. Alongside low magnetic susceptibility in sediments, this suggests erosion and episodes of lake desiccation due to reduced water availability (Table 1).

Sierra Madre Occidental.

5) Ciénega Las Taunas (1,700 m asl). Ortega-Rosas *et al.* (2008) analyzed a sedimentary record which extends back to 13 kyr. This region experiences summer rainfall associated with NAM and winter precipitation linked to Pacific frontal systems. Vegetation varies with elevation; in the lowlands of Las Taunas, Cyperaceae and Poaceae dominate, while at higher elevations, oak and pine-oak forests are present, with characteristic species including *Quercus arizonica, Q. coccolobifolia, Q. durifolia, Pinus chihuahuana, P. herrerae*, and *Cupressus arizonica.* Before the onset of the Holocene (~12 kyr), altitudinal shifts in forest communities of the Sierra Madre Occidental were detected relative to the present-day vegetation. For example, during the YD, *Abies* was found at elevations ~300 m lower than its current distribution. Meanwhile, *Quercus*, Asteraceae, and Poaceae were poorly represented, indicating that western Mexico experienced cooler and wetter conditions during this period due to a weakened NAM. This contrasts with the subsequent slight increase of *Quercus* in response to the warm and dry conditions characteristic of the Greenlandian (Middle Holocene).

6) Ciénega Tonibabi (780 m asl). Galaz-Samaniego *et al.* (2023) analyzed a sedimentary sequence which spans from 15.5 kyr to the present. The ciénega is surrounded by a mountainous area that reaches elevations up to 2,300 meters. The mean annual temperature and precipitation are 20.7 °C and 507 mm, respectively. Most rainfall occurs during the summer due to convective processes associated with NAM, although winter precipitation increases during El Niño years and decreases during La Niña years. Vegetation includes pine and pine-oak forests at higher elevations, and thorn scrub and/or grasslands at lower elevations. Also, some tropical species are found in the region. At the end of MIS 2 (15 kyr), the core's deepest section shows the highest proportion of arboreal taxa, with *Pinus* dominant in areas now covered by thorn scrub. *Quercus* is less frequent but still notable. Other temperate trees as *Abies*, *Picea*, *Juglans*, *Alnus*, *Arbutus*, *Lythrum*, and Caryophyllaceae are present in low amounts. Herbaceous taxa like Amaranthaceae, Ambrosiinae, Asteroideae, and Poaceae are scarce. Vegetation changes are observed during the Bølling-Allerød and Younger Dryas, but the most pronounced shift occurs at the Holocene onset, when temperate

trees, especially *Pinus*, decline, while Amaranthaceae, Ambrosiinae, and Poaceae increase. However, continued presence of *Alnus oblongifolia* and *Fraxinus* suggests winter precipitation remained important (Table 1).

Central-West (Table 2).

Table 2. Summary of the pollen records from the TMVB-West region for MIS 1, MIS 2, MIS 3 and associated climate drivers of vegetation changes. Site number correspond to those indicated in the sedimentary records section. ">" is used for "increase, "<" for decrease, T° for temperature, Pp for precipitation and NR refers to no record.

Site	Current vegetation (low-high altitudinal gradient)	MIS 1 (14 - 7.2 kyr) Pollen / Driver	MIS 2 (29 - 14 kyr) Pollen / Driver	MIS 3 (57 - 29 kyr) Pollen / Dirver
7	Halophytic grasslands, thorn forest, tropical deciduous forest, and mixed pine-oak forests	**NR** / Lake desiccation, < Pp	> *Alnus, Pinus, Abies*, Asteraceae, Pocaceae < *Quercus* / < T° < Pp, weak NAM. Southern migration of the ITCZ.	> *Quercus, Pinus* < Asteraceae, *Alnus* / > T° > Pp, strong NAM. Northern migration of the ITCZ.
8	Subtropical shrub, pine, oak and pine-oak forest, fir forest	> *Pinus*, *Abies* < Poaceae / > T° > Summer Pp	**Before LGM:** > *Pinus* < *Quercus*, *Alnus*, *Juniperus* **After LGM:** > *Alnus*, *Artemisia*, *Salix*, *Ambrosia* < *Pinus*, *Abies* / < T° > Winter Pp	> *Abies, Alnus, Fraxinus, Quercus, Juniperus*, *Artemisia*, *Ambrosia* and Poaceae < *Pinus* / > T° > Summer Pp
9	Subtropical shrub, pine, oak and pine-oak forest, fir forest	> *Quercus*, *Alnus*, Poaceae, *Abies* < *Pinus*, Asteraceae / > T° > Summer Pp, < Pp during Heinrich Event 0, > AMOC	**Before LMG** > *Pinus* < Poaceae **After LMG** > Poaceae < *Pinus* / < T° > Winter Pp < Pp during Heinrich Event 1, > AMOC	> *Pinus, Quercus, Alnus, Fraxinus*, Cupressaceae < *Abies* / > T° > Summer Pp, < Pp during Heinrich Events 5 and 4, > AMOC
10	Subtropical shrub, pine, oak and pine-oak forest, fir forest	> *Alnus, Quercus, Salix, Tilia, Abies, Platanus*, herbaceous taxa < *Pinus* / > T°, northern migration of the ITCZ	> *Pinus* < *Quercus, Alnu*s, herbaceous taxa / < T°, southern migration of the ITCZ	**NR**
11	Subtropical shrub, pine, oak and pine-oak forest, fir forest	> *Pinus, Alnus, Salix* < *Quercus*, *Ambrosia*, *Artemisia*, Poaceae / > T°, northern migration of the ITCZ	> Amaranthaceae, Asteraceae, Poaceae, *Alnus*, *Quercus*, *Cirsium* < *Pinus* / < T°, southern migration of the ITCZ	**Onset MIS 3** > *Ambrosia*, Amaranthaceae < *Alnus, Juglans, Fraxinus* **End MIS 3** > *Pinus, Alnus, Juglans Fraxinus* < *Ambrosia*, Amaranthaceae / > T°, northern migration of the ITCZ

7) Sayula (1,350 m asl). This record is the closest to the Pacific (Figure 3) and provides palynological information from 51 to 6 kyr (Rodríguez-Pérez 2018). The average annual temperature of the lake is 19.6 °C, and the average annual precipitation is 569 mm, mostly occurring between May and October. The vegetation in surrounding areas varies between halophytic grasslands, thorn forest, tropical deciduous forest, and mixed pine-oak forests (Table 2). Between 55-45 kyr, vegetation in the Sayula record was dominated by pine-oak forests with minor herbaceous elements like Poaceae and Asteraceae. During MIS 2, conditions shifted: 27-24 kyr was wetter, transitioning to drier conditions during the LGM. *Quercus* declined during the glacial phase, while *Alnus*, *Pinus*, and *Abies* increased. Herbaceous taxa peaked in abundance during the LGM (Rodríguez-Pérez 2018). After 18 kyr, pollen became scarce due to lake desiccation caused by drought, which hindered preservation of palynological material.

Michoacán-Guanajuato Volcanic Field.- Four analyzed sedimentary records come from the Michoacán-Guanajuato Volcanic Field, located a few kilometers from each other (Figure 3). Pátzcuaro, Zacapu, and Zirahuén lakes are volcanic, as Cuitzeo is of tectonic origin. The altitude of the volcanic lakes is close to 2,000 m asl, whereas the tectonic lake is at 1,700 m asl. However, the basins include mountains exceeding 3,000 m asl. The climate is temperate with summer rainfall (June-October), and average annual precipitation ranges between 700 and 1,100 mm, with Zirahuén being the wettest site and Cuitzeo the driest. During winter, occasional rainfall occurs due to polar winds. Precipitation is associated with the northward migration of ITCZ and the expansion of the Hadley Cell (Bradbury 2000). Humidity in this region primarily arrives from the easterly winds of the Gulf of Mexico, but Pacific-origin winds also play a role (Lozano-García *et al.* 2013). The mean annual temperature varies with altitude; higher-altitude sites record temperatures close to 10 °C, while lower-altitude areas reach 20 °C (Maza-Villalobos *et al.* 2014). Vegetation is described in S1.

8) Pátzcuaro (2,044 m asl). The record spans the last 44 kyr (Watts & Bradbury 1982). The oldest part of the record corresponds to MIS 3, marked by the presence of *Abies*, *Alnus*, *Fraxinus*, *Juniperus*, and *Quercus*. *Pinus* was generally low, except for brief increases. *Artemisia*, *Ambrosia*, and Poaceae were also common. At the onset of MIS 2, *Pinus* increased significantly, while *Quercus*, *Alnus*, and *Juniperus* declined. After the LGM, *Pinus* and *Abies* decreased, whereas *Alnus*, *Artemisia*, and *Salix* increased. During deglaciation, *Alnus* and Cupressaceae rose. Watts & Bradbury (1982) linked this to drought-tolerant *Juniperus*, suggesting cold and dry MIS 2 conditions. Bradbury (2000) challenged this, noting most Cupressaceae in the Central Mexican Plateau prefer summer rainfall, except *Cupressus californica*, found in Baja California. Late MIS 2 peaks in *Ambrosia* and *Artemisia* also suggest dry and cold conditions. At the onset of the Holocene, *Pinus* and *Abies* increased, as Poaceae declined (Table 2).

9) Zacapu (1,970 m asl). Located 27 km northwest of Pátzcuaro (Figure 3), covers the last 52 kyr (Xelhuantzi-López 1991, Correa-Metrio *et al.* 2012b), although this core exhibits a hiatus between 31 and 19 kyr. During MIS 3, *Pinus* was dominant but fluctuated, accompanied by *Quercus*, *Alnus*, *Fraxinus*, and Cupressaceae. During Heinrich Event 5, *Pinus*, Brassicaceae, and Poaceae increased, while the other taxa declined, but later returned to previous levels. A similar pattern occurred during Heinrich Event 4, with a sharp rise in Asteraceae. From 19 kyr, *Pinus* dominated over 80% of pollen, suggesting temperate conditions with low but not scarce precipitation, as grasslands did not replace pine forests. Toward the end of the LGM, *Pinus* declined and Asteraceae, Cyperaceae, and Poaceae increased (Xelhuantzi-López 1991, Correa-Metrio *et al.* 2012b). During Heinrich 1 (~16 kyr), cooling reduced *Quercus*, *Alnus*, *Fraxinus*, and Cupressaceae, while Poaceae and aquatic taxa rose. In the Bølling-Allerød (14-12 kyr), a rising of *Pinus* and decreasing of herbaceous and aquatic taxa was detected. In the Holocene, *Quercus* and *Alnus* increased, making *Pinus* less dominant (Correa-Metrio *et al.* 2012b, Table 2).

10) Zirahuén (2,075 m asl). Located 29 km and 42 km south of Pátzcuaro and Zacapu, respectively, pollen records from two sedimentary sequences spanning 17 kyr have been studied (Torres-Rodríguez *et al.* 2012, Lozano-García *et al.* 2013). Around 17 kyr, cold and dry conditions supported extensive pine forests, though typical LGM peaks in Asteraceae and Poaceae were absent (Torres-Rodríguez *et al.* 2012). Toward the end of deglaciation (13.5-12.1 kyr) at Zirahuén, *Quercus* and *Alnus* slightly increased (Torres-Rodríguez *et al.* 2012, Lozano-García *et al.* 2013). In the Holocene, dominant pollen taxa included *Pinus*, *Quercus*, and *Alnus*, with notable values for *Abies* and *Platanus*. Although Early Holocene forests were mostly *Pinus* and *Quercus*, the presence of *Alnus* and *Carpinus*

suggests increased humidity and a shift from the dry pine-dominated forests of the Pleistocene (Lozano-García *et al.* 2013, Table 2).

11) Cuitzeo (1,880 m asl). The sedimentary sequence extends up to approximately 120 kyr (Israde-Alcantara *et al.* 2010). During MIS 3, fluctuations in the arboreal component are observed. Around the middle of MIS 3 (~42 kyr), there is a considerable increase in herbaceous taxa such as *Ambrosia* and Amaranthaceae; however, arboreal pollen gradually increases again, particularly *Alnus*, *Salix*, *Juglans* and *Fraxinus*, suggesting a transition from a cold phase to warmer and more humid conditions toward the end of MIS 3. At the onset of MIS 2, increases in Amaranthaceae, Asteraceae, Poaceae, *Cirsium*, *Quercus* and *Thalictrum* are detected, alongside a decline in *Pinus*. LGM signal was characterized by low *Pinus* values contrasted with high counts of *Alnus*, *Quercus* and Poaceae (Israde-Alcantara *et al.* 2010). At the beginning of the Holocene, vegetation responses to rising temperatures are evident because *Pinus*, *Alnus* and *Salix* became significantly more abundant, as *Quercus*, *Ambrosia*, *Artemisia* and Poaceae decreased (Israde-Alcantara *et al.* 2010, Table 2).

Central-East (Table 3).

Table 3. Summary of the pollen records from the TMVB-East region for MIS 1, MIS 2, MIS 3, MIS 5e, MIS 6 and associated climate drivers of vegetation changes. Site number correspond to those indicated in the sedimentary records section. ">" is used for "increase, "<" for decrease, T° for temperature, Pp for precipitation and NR refers to no record.

Site	Current vegetation (low-high altitudinal gradient)	MIS 1 (14 - 7.2 kyr) Pollen / Driver	MIS 2 (29 - 14 kyr) Pollen / Driver	MIS 3 (57 - 29 kyr) Pollen / Dirver	MIS 5e (129 - 116 kyr) Pollen / Dirver	MIS 6 (146 - 129 kyr) Pollen / Dirver
12	Xerophytic scrub, pine-oak and Juniperus forest, pine-fir forest	> *Pinus, Abies* < *Quercus, Picea*, *Alnus, Ulmus* / > T°, northern migration of the ITCZ	> *Pinus*, Amaranthaceae < *Quercus* / < T°, southern migration of the ITCZ	> *Abies, Picea, Alnus*, Cupressaceae, *Quercus* < Herbaceous taxa / > T°, northern migration of the ITCZ	NR	NR
13	Xerophytic shrublands, Juniperus forest, cloud forest, pine-oak and pine-fir forest, subalpine grasslands	> *Quercus, Alnus, Abies* < Poaceae, Asteraceae, Amaranthaceae / > T°, northern migration of the ITCZ. > Pp, > Easterlies humidity	Before LMG: > *Quercus, Alnus, Fraxinus*, Cupressaceae < Pinus After LMG: > *Pinus*, Poaceae, Amaranthaceae, Asteraceae < *Quercus, Alnus, Fraxinus* / < T°, southern migration of the ITCZ. > Pr before LMG, drier after LMG, < Easterlies humidity	> *Pinus, Quercus, Alnus* < Poaceae / > T°, northern migration of the ITCZ. > Pp, > Easterlies humidity	NR	NR

Site	Current vegetation (low-high altitudinal gradient)	MIS 1 (14 - 7.2 kyr) Pollen / Driver	MIS 2 (29 - 14 kyr) Pollen / Driver	MIS 3 (57 - 29 kyr) Pollen / Dirver	MIS 5e (129 - 116 kyr) Pollen / Dirver	MIS 6 (146 - 129 kyr) Pollen / Dirver
14	Xerophytic shrublands, Juniperus forest, cloud forest, pine-oak and pine-fir forest, subalpine grasslands	> *Pinus*, *Alnus*, *Quercus*, *Abies* < Amaranthaceae, Asteraceae, Poaceae / > T° > Pp, > Easterlies humidity. Northern migration of the ITCZ	> *Alnus*, *Quercus*, *Mimosa*, Cupressaceae, Amaranthaceae, Asteraceae, Poaceae, *Artemisia* < *Pinus* / < T° < Pp, < Easterlies humidity. Southern migration of the ITCZ	> *Pinus*, *Abies*, *Quercus*, *Picea* < Herbaceous taxa / > T° > Pp, > Easterlies humidity. Northern migration of the ITCZ	> *Pinus*, < Poaceae, Asteraceae, Amaranthaceae / > T° > Pp, > Easterlies humidity. Northern migration of the ITCZ	> Poaceae, Asteraceae, Amaranthaceae < *Pinus* / < T° < Pr, < Easterlies humidity. Southern migration of the ITCZ
15	Oak, pine-oak, fir-pine and pine forest, alpine grassland	> Amaranthaceae, Asteraceae, Verbenacae, *Pinus*, *Picea* / > T° > Pp, > Easterlies humidity. Northern migration of the ITCZ	> Poaceae, Asteraceae < *Pinus*, *Quercus*, *Alnus*, *Abies* / < T° < Pp, < Easterlies humidity. Southern migration of the ITCZ	NR	NR	NR

12) Jalapasquillo crater (2,400 m asl). The sequence spans from 35 to 8 kyr (Straka & Ohngemach 1989). Currently, the vegetation surrounding the crater consists of xerophytic scrub with *Nolina, Quercus, Agave, Hechtia, Juniperus* and Cactaceae. In nearby higher-altitude areas (*i.e.*, Las Derrumbadas), forest elements such as *Pinus*, *Quercus* and *Juniperus* are present (Moctezuma *et al.* 2016). Less than 30 km away is Pico de Orizaba, where pine and fir forests are found (Ávila *et al.* 1994). Around 33 kyr (MIS 3-2 transition), pine-oak forests dominated, with limited presence of *Abies*, *Picea*, *Alnus*, and Cupressaceae. Herbaceous taxa were sparse. During the LGM, *Quercus* declined, while *Pinus* and *Amaranthaceae* increased. By late MIS 2, *Pinus* dominated as other trees declined. In the early Holocene, vegetation was mostly *Pinus* and *Abies*; taxa as *Quercus*, *Picea*, *Alnus*, *Fagus*, and *Juglans* became scarce or vanished (Straka & Ohngemach 1989, Table 3).

Basin of Mexico.- One of the most extensively studied paleoecological regions is BM, where sedimentary records from Lakes Tecocomulco, Texcoco and Chalco reveal vegetation history dating back 150 kyr (Lozano-García *et al.* 1993, 2022, Lozano-García & Ortega-Guerrero 1998, Caballero *et al.* 1999). South of BM lie Lakes Texcoco and Chalco (Figure 3). The altitude in this area is 2,330 m asl, with a present-day mean annual temperature of approximately 14 °C and an annual precipitation ranging between 537 and 596 mm, with the most significant rainfall occurring from June to September due to ITCZ migration (Lozano-García & Ortega-Guerrero 1998). The vegetation of the BM is described in S1.

13) Texcoco (2,330 m asl). The pollen record from Texcoco shows that between 35 and 23 kyr, *Pinus*, *Quercus*, and *Alnus* were dominant, with occasional grains of *Carpinus*, *Carya*, *Fagus*, *Ilex*, *Juglans*, *Liquidambar*, *Podocarpus*, *Thalictrum*, *Ulmus*, and *Engelhardtia*; typical taxa of humid environments. *Poaceae* was scarce. Around 25 kyr, *Pinus* declined sharply, while *Quercus*, *Alnus*, *Fraxinus*, and Cupressaceae increased, indicating more humid

conditions (Lozano-García & Ortega-Guerrero 1998). During the LGM (22.8-18 kyr), drier conditions prevailed, with pine forests expanding and most trees decreasing, except *Abies*, *Picea*, and *Podocarpus*. Similar drought and cooling signals appeared north of BM, marked by reduced tree cover and increased *Poaceae* and *Amaranthaceae* (Caballero *et al.* 1999). By mid-MIS 2 (19-15 kyr), *Poaceae*, *Amaranthaceae*, and *Asteraceae,* characteristic of cold and dry zones, dominated the record. At the Holocene, warming and wetter conditions led to grasslands retreating uphill, while *Quercus*, *Alnus*, and *Abies* increased in lower areas (Lozano-García & Ortega-Guerrero 1998, Table 3).

14) Chalco (2,250 m asl). The record of this site is composed of several sequences studied by Lozano-García *et al.* 1993, Lozano-García & Ortega-Guerrero 1994, Lozano-García & Ortega-Guerrero 1998 and Lozano-García *et al.* 2022. Early studies covered MIS 2 and MIS 1, while recent work extends to MIS 6 (146-126 kyr). MIS 6 vegetation was mostly herbaceous, dominated by Poaceae, Amaranthaceae, and Asteraceae, with some sparse arboreal taxa like Cupressaceae, *Quercus*, and *Pinus*. Taxon richness was highest during MIS 6 due to low *Pinus* dominance (Lozano-García *et al.* 2022). During MIS 5e (Eemian, 129-116 kyr), warming favored *Pinus*, *Abies*, and *Picea* forests, alongside tropical taxa such as *Arctostaphylos*, *Cecropia*, *Arecaceae*, and *Myrtaceae*, and mesophytic trees like *Carya*, *Carpinus*, *Juglans*, *Myrica*, *Podocarpus* and *Tilia*. After this warm period, colder conditions returned in MIS 5d, with herbaceous plants dominating again, but some MIS 6 grassland taxa did not recover. By the end of MIS 5d (116-108 kyr), *Pinus* increased at the expense of *Alnus*, *Quercus*, and mesophytic taxa. Extensive pine forests established from MIS 5b (92-86 kyr) to the present. During MIS 3, *Pinus* remained dominant, except during Heinrich events 5 and 4 when *Abies*, *Quercus*, and *Picea* increased. Herbaceous taxa like *Artemisia* and *Poaceae* peaked as *Pinus* declined. At the onset of MIS 2, *Pinus* declined toward the LGM while *Alnus*, *Quercus*, and *Cupressaceae* rose. Post-LGM, *Mimosa* and *Cupressaceae* increased. Around Bølling-Allerød (14 kyr), *Carpinus*-*Corylus* and *Cirsium* increased. In the Holocene, *Pinus* and *Alnus* rose, herbaceous plants declined, and later *Alnus* fell as *Abies* and *Quercus* increased (Lozano-García *et al.* 1993, Lozano-García & Ortega-Guerrero 1994, Table 3).

15) Chignahuapan, Lerma Basin (2,570 m asl). The core covers the last 23 kyr, making it the highest-altitude site in Central Mexico. Currently, this site is considered to have a temperate climate with summer rainfall, an average annual temperature of 12.2 °C, and an average annual precipitation of 933 mm (Lozano-García *et al.* 2005). The highest point in the basin is Nevado de Toluca, at 4,680 m asl, where the significant elevation gradient promotes substantial vegetation turnover (S2). Between 21 and 16 kyr, during the peak of mountain glaciers (Lachniet & Vázquez-Selem 2005), herbaceous plants as Poaceae and Asteraceae were abundant. Arboreal taxa were scarce, with *Pinus*, *Quercus*, *Alnus*, *Cupressaceae*, and *Abies* being the main trees (Lozano-García *et al.* 2005). During deglaciation (16-11.85 kyr), *Poaceae* declined while herbaceous plants from *Amaranthaceae*, *Asteraceae*, *Verbenaceae*, and *Artemisia* increased, alongside *Pinus*, *Quercus*, and *Alnus*. At the onset of the Holocene, *Pinus* rose significantly, while *Quercus* and *Alnus* declined. *Abies* was absent, but *Picea* appeared in the record around 9 kyr. Herbaceous plants decreased notably compared to earlier periods (Lozano-García *et al.* 2005).

Southern region (Table 4). There are no sedimentary records in southern Mexico that cover glacial periods, but there are two in Yucatán Peninsula, Guatemala (Figure 3). Much of the region is characterized by low elevations but some mountains in the region reach up to 600 m asl. The mean annual temperature is 25 °C, and the mean annual precipitation is 1600 mm, although extreme years range from 900 mm/a to 2500 mm/yr. During summer, the northward position of ITCZ induces heavy rainfall in this region, facilitated by CLLJ, which transports significant moisture from the AWP to the Yucatán Peninsula. Within the rainy season, July and August are relatively drier due to *Canícula*. In winter, rainfall is scarce, although it can occur due to cold fronts known as *Nortes* (Correa-Metrio *et al.* 2012a). The vegetation in this region is highly diverse and can be classified into evergreen tropical forest, deciduous tropical forest, and semi-deciduous tropical forest (S2, Table 4).

16) Quexil (110 m asl). Leyden *et al.* (1993, 1994) analyzed sediments dating back to 36 kyr. From the base to 24 kyr, *Pinus*, *Quercus*, and *Alfaroa* dominated, alongside arboreal families like *Cupressaceae* and *Onagraceae*, and genera such as *Betula*, *Carpinus*, *Cornus*, *Fraxinus*, and *Juglans*. Herbaceous and tropical rainforest taxa were scarce or absent, indicating cooler, drier conditions favoring pine-oak forests in lowlands. Between 24 and 14 kyr,

arboreal taxa declined sharply except *Cupressaceae*, and herbaceous taxa as *Malvaceae*, *Poaceae*, *Amaranthaceae*, and *Cactaceae* became dominant, reflecting temperate thorn scrub replacing pine-oak during the LGM. Temperatures were 6.5-8 °C cooler than today. From 14 to 10.5 kyr, herbaceous plants prevailed, but humid taxa like *Alfaroa*, *Liquidambar*, *Quercus*, and *Ulmus* increased. After 10.5 kyr (Holocene onset), *Pinus* and *Quercus* rose rapidly, then declined as humid rainforest taxa became dominant (Table 4).

17) Petén Itza (100 m asl). Correa-Metrio *et al.* (2012a) and Cruz-Silva (2018) studied the pollen composition of Lake Petén Itzá. Cruz-Silva (2018) covers 250 to 85 kyr, while Correa-Metrio *et al.* (2012a) analyze the record from the 86 kyr to the present. Cruz-Silva's chronology reconstructs pollen composition back to the MIS 7 interglacial (243-191 kyr). During MIS 6 (191-129), warm and humid taxa like Moraceae, *Alchornea*, *Begonia*, *Brosimum, Ficus*, *Psychotria*, *Spondias* and *Trema* decline, while cooler indicators like *Alnus*, *Ambrosia*, *Myrica*, *Quercus*, Poaceae, and especially *Pinus* increase. Pines, previously scarce, become constant and fluctuate with temperature changes. The Eemian warming (MIS 5e, 129-116 kyr) triggered a sharp rise in Moraceae and a drop in *Pinus*. *Celtis* and Melastomataceae decline in MIS 5d (116 to 108 kyr) but rise again in MIS 5c (108-92 kyr). During MIS 3, arboreal and non-arboreal taxa alternate; *Pinus*, *Quercus*, and *Celtis* increase as Poaceae decreases, and vice versa. At the end of MIS 3, Pinus drops while *Ambrosia* and *Eugenia* rose. Correa-Metrio *et al.* (2012a) suggest dry summers with winter rains at MIS 2 onset, with temperate forests dominated by *Juglans*, *Myrica*, *Quercus*, and *Pinus*. Between 18.5 and 10.5 kyr, tropical dry taxa like *Acacia*, *Bursera*, *Celtis*, *Mimosa*, and *Sapium* rose, and during the Holocene transition, tropical dry forests further expand as indicated by increased abundances of *Brosimum*, *Bursera*, *Cecropia*, *Ficus*, *Trema* and Moraceae in the record (Table 4).

Table 4. Summary of the pollen records from the South region for MIS 1, MIS 2, MIS 3, MIS 5e, MIS 6 and associated climate drivers of vegetation changes. Site number correspond to those indicated in the sedimentary records section. ">" is used for "increase, "<" for decrease, T° for temperature, Pp for precipitation and NR refers to no record.

Site	Current vegetation (low-high altitudinal gradient)	MIS 1 (14 - 7.2 kyr)Pollen / Driver	MIS 2 (29 - 14 kyr) Pollen / Driver	MIS 3 (57 - 29 kyr) Pollen / Dirver	MIS 5e (129 - 116 kyr) Pollen / Dirver	MIS 6 (191 - 129 kyr) Pollen / Dirver
16	Semi-deciduous tropical forest, deciduous tropical forest, evergreen tropical forest	> *Alfaroa*, *Quercus*, *Ulmus*, *Liquidambar*, Amaranthaceae < Poaceae / > T°, > spring isolation > Summer Pp	> Poaceae, Malvaceae, Amaranthaceae, Cupressaceae < *Pinus*, *Quercus*, *Juglans* / < T°, < maximum isolation < Summer Pp	> *Pinus*, *Quercus*, *Alfaroa*, Cupressaceae, Onagraceae, *Carpinus* < Malvaceae, Amaranthaceae / > T°, > spring isolation > Summer Pp	NR	NR
17	Semi-deciduous tropical forest, deciduous tropical forest, evergreen tropical forest	> *Brosimum*, *Bursera*, *Cecropia*, *Ficus*, *Trema*, Moraceae, *Begonia* < Asteraceae, *Alnus*, *Celtis*, *Pinus* / > T°, > seasonality isolation. > Summer Pp, drier conditions during Heinrich Event 0, > AMOC. Northern migration of the ITCZ	> *Juglans*, *Myrica*, *Quercus*, *Alnus*, *Pinus* < *Celtis* / < T°, < seasonality isolation. < Summer Pp, > Winter Pp, cold fronts, drier conditions during Heinrich Event 2 and 1, > AMOC. Southern migration of the ITCZ	> *Celtis*, *Pinus*, Poaceae, *Quercus* < Convolvulaceae, Melastomataceae / > T°, > seasonality isolation. > Summer Pp, drier conditions during Heinrich Events 5-3, > AMOC. Northern migration of the ITCZ	> Moraceae < *Pinus* / > T° < Pp, northern migration of the ITCZ	> *Alnus*, *Ambrosia*, *Myrica*, *Quercus*, Poaceae, *Pinus* < Moraceae, *Alchornea*, *Begonia*, *Ficus*, *Trema* / < T° < Summer Pp, southern migration of the ITCZ > Winter Pp, cold fronts

Meta-analysis results

The meta-analysis detected significant heterogeneity among sites, which justifies the use of a multivariate random-effects model ($\sigma^2 = 0.0115$). The set of moderators used (MIS, Region, Elevation, Elevational Range, and the interaction between the last two) significantly explained the variability in the effects of changes in arboreal pollen proportion ($QM_{12} = 433.09$; $P < 0.0001$).

Changes in arboreal pollen among the MISs showed significant differences (Table 5). MIS 1 exhibited a 2.14 and 2.27 % lower proportion of arboreal pollen than MIS 2 and MIS 3, respectively ($P = 0.0012$ and 0.0009, respectively), while no significant differences were observed between MIS 3 and MIS 2 ($P = 0.77$). Both MIS 5e and MIS 6 exhibited significantly lower percentages of arboreal pollen compared to MIS 2 (by 7.07 and 17.15 %, respectively; $P < 0.0001$ in both cases). MIS 5e had approximately 5 % less arboreal pollen than MIS 1 and 7 % less than MIS 3 ($P < 0.0001$ for both comparisons). When comparing MIS 5 and MIS 6, it was observed that during the glacial stage (MIS 6), there was approximately 10 % less arboreal pollen than during the interglacial stage ($P < 0.0001$), indicating that MIS 6 had the highest proportion of herbaceous taxa (Table 5).

Table 5. Comparison of arboreal pollen percentage among Marine Isotope Stages (MISs). The upper triangle of the matrix presents adjusted p-values for each comparison; the lower triangle shows the relative changes in arboreal pollen percentage. Values in brackets represent the lower and upper bounds of the confidence intervals.

MIS	MIS 1	MIS 2	MIS 3	MIS 5e	MIS 6
MIS 1	X	$P = 0.0012$	$P = 0.0009$	$P < 0.0001$	$P < 0.0001$
MIS 2	0.0214 (0.0091, 0.0336)	X	$P = 0.7748$	$P < 0.0001$	$P < 0.0001$
MIS 3	0.0227 (0.0103, 0.0351)	0.0013 (-0.0078, 0.0105)	X	$P < 0.0001$	$P < 0.0001$
MIS 5e	-0.0493 (-0.0695, -0.0292)	-0.0707 (-0.0893, -0.0522)	-0.0720 (-0.0890, -0.0550)	X	$P < 0.0001$
MIS 6	-0.1501 (-0.1712, -0.1289)	-0.1715 (-0.1911, -0.1518)	-0.1728 (-0.1909, -0.1546)	-0.1007 (-0.1217, -0.0798)	X

Strong regional differences in arboreal pollen percentages were also observed (Table 6). Among the northern regions (Chihuahuan Desert, Sonoran Desert and Sierra Madre Occidental [SMO]), the Sonoran Desert significantly differed from the rest. The Chihuahuan Desert had the highest percentage of arboreal pollen, showing 78 % higher than the Sonoran Desert ($P = 0.0006$). Even though Chihuahuan Desert arboreal pollen percentage was 45 % higher than the SMO, no significant differences were found after adjusting p-values ($P = 0.0622$). The TMVB East region exhibited a distinct response from TMVB West and Southern regions regarding arboreal pollen. The eastern region had 1.8 times more arboreal pollen than the western region ($P = 0.0466$). The southern region, meanwhile, had 2.3 times less arboreal pollen than TMVB-East ($P = 0.0466$), but did not differ significantly from TMVB-West (-50.52 %, $P = 0.0698$).

Topographic variables indicated that elevation was positively associated with arboreal pollen percentage (0.0004, $P = 0.0508$). This trend suggested an increase of 0.0004 % in arboreal pollen proportion for each additional meter in elevation. Therefore, an increase of 1,000 meters results in a 0.4 % rise in arboreal pollen. Similarly, elevational range was also positively associated with arboreal pollen percentage (0.0004, $P < 0.0001$), indicating that greater altitudinal heterogeneity was linked to higher arboreal pollen values. However, the interaction between these two

variables reduced their positive effects beyond a certain threshold (-0.0000, $P = 0.0056$) (Figure 4). Thus, in sites with high elevational range, the positive effect of elevation was diminished or may even become negative, whereas, in areas with low elevational range, elevation maintained a positive effect on arboreal pollen percentage.

Discussion

The meta-analysis allowed us to identify changes in vegetation composition based on palynological records across different MISs and regions, as well as to evaluate the effects of topographic variables on vegetation patterns. It is important to emphasize that the obtained results fundamentally depend on the chronologies reported in the referenced studies; therefore, future advances in sediment dating could significantly alter the results presented here.

Although all records showed substantial changes in pollen assemblages between glacial and interglacial stages, it is essential to assess the directionality of these changes from a macroregional perspective. In both glacial-interglacial cycles analyzed (MIS 6-MIS 5 and MIS 2-MIS 1), arboreal pollen percentages significantly increased during interglacial periods (Figure 1, Table 5). Correa-Metrio *et al.* (2012a) refers to these as "press-driven changes," linked to variations in Earth's orbital parameters that modulate the migration of the ITCZ. By contrast, MIS 3 did not differ significantly from MIS 2, which may reflect the high climatic variability characteristic of MIS 3 (Figure 2). This interval includes Heinrich Events 5 and 4 (Figure 2), marked by especially cold and dry conditions due to fluctuations in the AMOC, and associated with abrupt changes in pollen composition across several regions (Correa-Metrio *et al.* 2012a, b). Such vegetation shifts are identified as "pulse-driven changes", indicating short-term perturbations after which previous conditions may be re-established. Differences between MIS 5e and MIS 1 should be interpreted with caution, since the meta-analysis only the Chalco study covers this temporal range (Lozano-García *et al.* 2022). Nevertheless, Cruz-Silva (2018) reports high Moraceae counts in the Petén Itzá record between MIS 6 and MIS 5e, along with a decline in *Celtis* and Melastomataceae, suggesting that the arboreal pollen response may be consistent with the pattern observed in Chalco.

Regional contrast in arboreal pollen percentages also provided key insights for paleoclimatic interpretation (Figure 1). The differences among sites in the northern region may be related to differences in elevation and topographic heterogeneity (Tables 1 and 2, Figure 4,). For example, Sonoran Desert sites are located below 1,500 m asl, whereas the Chihuahuan Desert site is at 2,138 m asl, and the SMO site at 780 m asl. The interaction between elevation and

Table 6. Comparison of arboreal pollen percentages among regions. The upper triangle of the matrix presents adjusted p-values for each comparison; the lower triangle shows the relative changes in arboreal pollen percentage. Values in brackets represent the lower and upper bounds of the confidence intervals. Only regions influenced by climatic drivers in common were compared (Tables 1-4).

Regions	Chihuahuan Desert	Sonoran Desert	Sierra Madre Occidental	TMVB West	TMVB East	South
Chihuahuan Desert	X	$P = 0.0006$	$P = 0.0622$	X	X	X
Sonoran Desert	-0.7891 (-1.1961, -0.3821)	X	$P = 0.0466$	X	X	X
Sierra Madre Occidental	-0.4525 (-0.8639, -0.410)	0.3367 (0.0589, 0.6144)	X	X	X	X
TMVB West	X	X	X	X	$P = 0.0466$	$P = 0.0698$
TMVB East	X	X	X	1.8195 (0.2879, 3.3510)	X	$P = 0.0466$
South	X	X	X	-0.5052 (-1.0513, 0.0409)	-2.3247 (-4.2471, -0.4023)	X

elevational range appears to strongly influence arboreal pollen values at Alta Babícora, highlighting the role of "sky islands," as refugia for arboreal elements during interglacial periods (Mastretta-Yanes *et al.* 2015, Galaz-Samaniego *et al.* 2023). The northern paleoclimatic responses showed and increment in precipitation during glacial phases due to a strong thermal gradient in the Pacific, which causes the Westerlies to suppress NAM (Figure 1). In contrast, drier conditions prevail during last interglacial (MIS 1), as the thermal gradient weakens, shifting precipitation to higher latitudes (Bhattacharya *et al.* 2018). A clear example of this process is drying of San Felipe and Alta Babícora lakes at the onset of the Holocene, leading to the establishment of unprecedented desert communities in the region (Table 1).

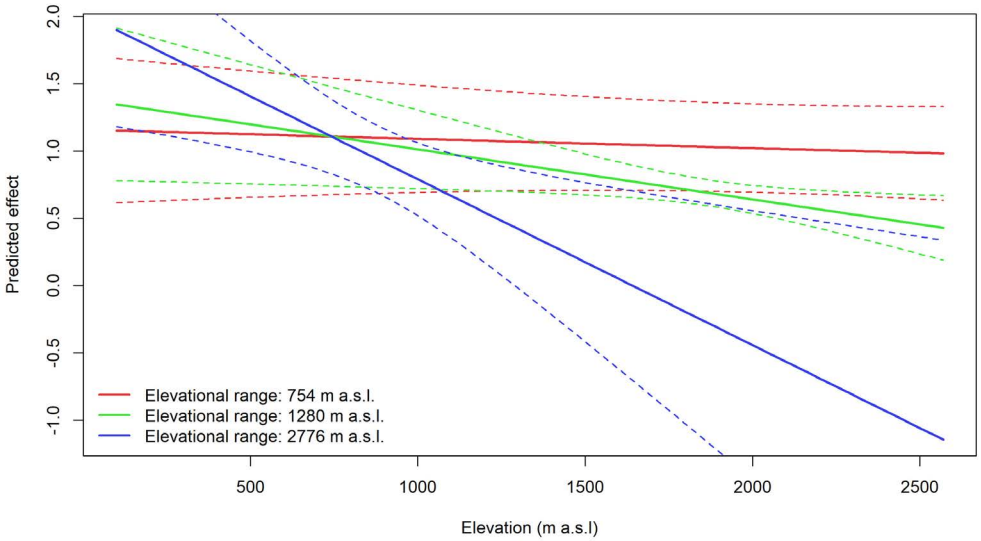

Figure 4. Responses of arboreal pollen to the interaction between elevation and elevational range based on the meta-analysis. The X-axis represents elevation, while the Y-axis shows the predicted effect of elevation under three elevational range scenarios: low (first quartile, red), medium (second quartile, green), and high (third quartile, blue).

An important difference was observed between the two sectors of the TMVB. Although mixed forests were identified in both regions, the eastern sector exhibited a higher percentage of arboreal pollen than the western sector. The main difference between TMVB subregions was associated with elevational contrast (Figure 3, Table 6, Caballero *et al.* 2010). In the west, mountain ranges are lower in elevation than those in the east. A key factor for TMVB precipitation is the ITCZ latitudinal migration and the effects of the CLLJ (Figure 1, Lozano-García & Ortega-Guerrero 1998, Metcalfe *et al.* 2015, Lozano-García *et al.* 2022). During cold periods such as Last Glacial Maximum (MIS 2), it is likely that warm air from the Gulf of Mexico cooled at lower altitudes, triggering convective processes in lowland areas (Correa-Metrio *et al.* 2012b). Different responses from vegetation to climate were observed in TMVB-West region (Tables 2, 5 and 6), suggesting that changes depend on local variations (Lozano-García *et al.* 2013). During MIS 2, winters were wetter in the central-western region, reducing the seasonal contrast between summer and winter precipitation compared to present-day conditions (Bradbury 2000). Although there is still debate about the mechanism that favors winter rainfall in glacial periods, the proposed mechanism suggests that increased ice cover weakened the NPH, allowing moisture-laden winds to reach farther south (Bradbury 2000). However, greater attention should be paid on cold fronts rainfall. Correa-Metrio *et al.* (2012b) expanded on this explanation, proposing that summers during MIS 2 were cold and particularly dry. Due to regional temperature reductions, warm, humid winds from the Gulf of Mexico formed clouds over lower-altitude mountains in the east, which acted as barriers preventing moisture from reaching the western region. Therefore, winter rainfall was crucial in avoiding severe droughts in western central Mexico. As a consequence, precipitation decreases during glacials and increases during interglacials, which is associated with the northward shift of ITCZ and the greater intensity of the Easterlies. As humidity and

temperature patterns changed, plant communities migrate along the elevational gradient until the next glacial cycle. Between glacials, species composition continued changing, with local extinctions and new taxa colonized (Lozano-García *et al.* 2022).

The lack of significant differences in arboreal pollen percentage in the meta-analysis between the South and TMVB-West, SMO and Chihuahuan desert should be considered as not representative because of evident vegetation changes. During glacial periods, southern vegetation is characterized by elements typical of temperate forests, whereas tropical forest elements predominate during interglacial periods (Table 4). The south region climate variations are strongly linked to ITCZ migration. During summer, the northward migration of the ITCZ causes NASH to shift, and the Easterlies to weaken, facilitating precipitation. In contrast, during winter the ITCZ moves southward, lowering air temperature and increasing ocean surface pressure, creating an anticyclonic zone with strong winds in the Caribbean (Correa-Metrio *et al.* 2012a, Figure 1).

The negative interaction between physiographic variables can be explained by the presence of alpine grasslands at the highest elevations, especially in the eastern TMVB, which reduce arboreal pollen representation. This coincides with glacial geomorphology records from the mountains of central Mexico which indicate that during LGM, the equilibrium line of glaciers descended overall. However, though the extent varied between the central and central-western regions. In the more humid central-western region, where glaciers no longer exist, moraines have been found at approximately 3,400 m asl., while in the Iztaccíhuatl (central Mexico), they reached 3,940 ± 130 m asl (currently at 4,970 ± 90 m asl). This shift also lowered the tree line (Lachniet & Vázquez-Selem 2005, Vázquez-Selem & Heine 2011). Temperature is estimated to have decreased by 5 to 9 °C in central Mexico compared to present-day conditions (Vázquez-Selem & Heine 2011). For example, in the Chignahuapan record, peaks in herbaceous taxa, mainly Poaceae, during MIS 2 correlate directly with glacial advances. Meanwhile, overall humidity in the central region declined during LGM (Tables 3 and 4); although summer droughts prevailed due to the suppression of the Easterlies, winter precipitation likely increased. Conversely, it has been observed that, at the onset of the Holocene, the equilibrium line of the glaciers rose, allowing arboreal elements to expand to higher elevations at the expense of a decrease in herbaceous plants (Lozano-García & Vázquez-Selem 2005).

Throughout paleoclimatic records, vegetation turnover in response to climate variations is evident (Tables 1-6). Based on the analyzed records, two types of vegetation migration during abrupt environmental changes can be observed: latitudinal shifts in southern records and altitudinal shifts in central sites. These processes are detectable synchronously in nearby locations. The difference between migration types is attributed to the rugged topography of the FVTM, which acts as a barrier to dispersion (Guzmán-Vázquez *et al.* 2023). Various ecological factors such as seed production and dispersal, germination and seedling development, and species interactions, alongside climatic factors, play a crucial role in determining whether a species establishes itself in a new location (Guzmán-Vázquez *et al.* 2023).

According to the ecological niche theory (Whittaker *et al.* 1973), living organisms have both upper and lower environmental limits for survival. In terrestrial plants, two key variables determine their fundamental niche: temperature and precipitation, both exhibited significant fluctuations throughout the Quaternary (Figure 2). During this period, large-scale global environmental changes drove plant communities to adapt to new conditions. The possible responses of plants to climate change range from expanding their tolerance range *in situ*, to migrating altitudinally or latitudinally (Figure 4), or becoming extinct if conditions become too extreme. As a result, plant communities are dynamic over time (Jackson & Overpeck 2000). During glacial and interglacial periods, vegetation composition and structure changed, favoring certain species that expanded their range under new environmental conditions, while others became restricted to small refugia - also called microrefugia - or even faced local extinction (Leyden *et al.* 1994, Mastretta-Yanes *et al.* 2015). This dynamic process leads to constant species reassembly, forming different spatial and temporal species assemblages.

Under the current warming scenario, plant migration processes along elevational gradients have been documented, showing that some cloud forest species are moving upslope to compensate for thermal and water stress, while heat-tolerant species are shifting downslope (Ramírez-Barahona *et al.* 2025).

A recurring feature in the analyzed records is the presence of non-analog communities: assemblages that differ compositionally from any present-day ecosystems. These communities may be affected by climatic forces that no longer exist today (Williams & Jackson 2007). Given the progressive warming scenarios in the era of greenhouse gases, unprecedented communities will likely become more common in historical records. This underscores the need for conservation strategies that incorporate topographic diversity as a central element in addition to considering alpha and beta diversity.

Supplementary material

Supplemental data for this article can be accessed here: https://doi.org/10.17129/botsci.3738

Acknowledgments

Manuel Zepeda Pirron thanks the Posgardo en Ciencias de la Tierra, UNAM and SECIHTI (CVU 1085983) for financial support. We thank Susana Sosa Najera for her support in obtaining several of the databases used in this meta-analysis and for the suggestions throughout this research. We also thank Blanca Lorena Figueroa Rangel for her valuable comments and suggestions regarding the structure of this manuscript, and an anonymous reviewer.

Literature cited

Ávila CH, Aguirre JR, Garcia E. 1994. Fir (*Abies hickelii* Flous & Gaussen) forest structure variation in relation to environmental factor on the Orizaba Peak, Mexico. *Forest Systems* **3**: 5-17. DOI: https://doi.org/10.5424/516

Bhattacharya T, Tierney JE, Addison JA, Murray JW. 2018. Ice-sheet modulation of deglacial North American monsoon intensification. *Nature Geoscience* **11**: 848-852. DOI: https://doi.org/10.1038/s41561-018-0220-7

Björck S, Walker MJC, Cwynar LC, Johnsen S, Knudsen KL, Lowe JJ, Wohlfarth B. 1998. An event stratigraphy for the last termination in the North Atlantic region based on the Greenland ice-core record: a proposal by the INTIMATE group. *Journal of Quaternary Science* **13**: 283-292. DOI: https://doi.org/10.1002/(SICI)1099-1417(199807/08)13:4<283::AID-JQS386>3.0.CO;2-A

Boos WR, Pascale S. 2021. Mechanical forcing of the North American monsoon by orography. *Nature* **599**: 611-615. DOI: https://doi.org/10.1038/s41586-021-03978-2

Bradbury JP. 2000. Limnologic history of Lago de Pátzcuaro, Michoacán, México for the past 48,000 years: impacts of climate and man. *Paleogeography, Paleoclimatology, Palaeoecology* **163**: 65-95. DOI: https://doi.org/10.1016/S0031-0182(00)00146-2

Broccoli AJ, Dahl KA, Stouffer RJ. 2006. Response of the ITCZ to Northern Hemisphere cooling. *Geophysical Research Letters* **33**: L01702. DOI: https://doi.org/10.1029/2005GL024546

Broecker WS, Peteett DM, Rindt D. 1985. Does the ocean-atmosphere system have more than one stable mode of operation? *Nature* **315**: 21-26. DOI: https://doi.org/10.1038/315021a0

Brunelle A, Carter VA, Delgadillo Rodríguez J, Feagin V, Watt J. 2024. A late glacial paleoenvironmental and climate record from the Sierra de Juarez, Baja California. *Quaternary International* **705**: 94-103. DOI: https://doi.org/10.1016/j.quaint.2024.06.013

Buizert C, Adrian B, Ahn J, Albert M, Alley RB, Baggenstos D, Bauska TK, Bay RC, Bencivengo BB, Bentley CR, Brook EJ, Chellman N J, Clow GD, Cole-Dai, J, Conway H, Cravens E, Cuffey, KM, Dunbar NW, Edwards JS, Woodruff TE. 2015. Precise interpolar phasing of abrupt climate change during the last ice age. *Nature* **520**: 661-665. DOI: https://doi.org/10.1038/nature14401

Byrne MP, Pendergrass AG, Rapp AD, Wodzicki KR. 2018. Response of the Intertropical Convergence Zone to Climate Change: Location, Width, and Strength. *In:* Chadwick R. ed, *Current Climate Change Reports*. **4***:* 355-370. DOI: https://doi.org/10.1007/s40641-018-0110-5

Caballero M, Lozano-García S, Ortega-Guerrero B, Correa-Metrio A. 2019. Quantitative estimates of orbital and millennial scale climatic variability in central Mexico during the last ~40,000 years. *Quaternary Science Reviews* **205**: 62-75. DOI: https://doi.org/10.1016/j.quascirev.2018.12.002

Caballero M, Lozano-García S, Ortega B, Urrutia J, Macias JL. 1999. Environmental characteristics of Lake Tecocomulco, northern basin of Mexico, for the last 50,000 years. *Journal of Paleolimnology* **22**: 399-411. DOI: https://doi.org/10.1023/A:1008012813412

Caballero M, Lozano-García S, Vázquez-Selem L, Ortega B. 2010. Evidencias de cambio climático y ambiental en registros glaciales y en cuencas lacustres del centro de México durante el último máximo glacial. *Boletín de La Sociedad Geológica Mexicana* **62**: 359-377. DOI: https://doi.org/10.18268/BSGM2010v62n3a4

Chen N, Thual S, Stuecker MF. 2019. El Niño and the Southern Oscillation: Theory. *Reference Module in Earth Systems and Environmental Sciences*. DOI: https://doi.org/10.1016/b978-0-12-409548-9.11765-8

Cheng W, MacMartin DG, Kravitz B, Visioni D, Bednarz EM, Xu Y, Luo Y, Huang L, Hu Y, Staten PW, Hitchcock P, Moore JC, Guo A, Deng X. 2022. Changes in Hadley circulation and intertropical convergence zone under strategic stratospheric aerosol geoengineering. *Npj Climate and Atmospheric Science* **5**: 32. DOI: https://doi.org/10.1038/s41612-022-00254-6

Chiang JCH, Friedman AR. 2012. Extratropical cooling, interhemispheric thermal gradients, and tropical climate change. *Annual Review of Earth and Planetary Sciences* **40**: 383-412. DOI: https://doi.org/10.1146/annurev-earth-042711-105545

Correa-Metrio A, Bush MB, Cabrera KR, Sully S, Brenner M, Hodell DA, Escobar J, Guilderson T. 2012a. Rapid climate change and no-analog vegetation in lowland Central America during the last 86,000 years. *Quaternary Science Reviews* **38**: 63-75. DOI: https://doi.org/10.1016/j.quascirev.2012.01.025

Correa-Metrio A, Lozano-García S, Xelhuantzi-López S, Sosa-Nájera,S, Metcalfe SE. 2012b. Vegetation in western Central Mexico during the last 50 000 years: Modern analogs and climate in the Zacapu Basin. *Journal of Quaternary Science* **27**: 509-518. DOI: https://doi.org/10.1002/jqs.2540

Cruz-Silva E. 2018. *Historia de la vegetación de la Península de Yucatán durante los últimos dos ciclos interglacial-glacial del Pleistoceno*. MSc Thesis. Universidad Nacional Autónoma de México.

Dansgaard W, Johnsen SJ, Clausen HB, Dahl-Jensen D, Gundestrup NS, Hammer CU, Hvidberg CS, Steffensen JP, Sveinbjörnsdottir AE, Jouzel J, Bond G. 1993. Evidence for general instability of past climate from a 250-kyr ice-core record. *Nature*, **364**: 218-220. DOI: https://doi.org/10.1038/364218a0

Emile-Geay J, Cobb KM, Carre M, Braconnot P, Leloup J, Zhou Y, Harrison SP, Corrège, T, McGregor HV, Collins M, Driscoll R, Elliot M., Schneider B, Tudhope A. 2016. Links between tropical Pacific seasonal, interannual and orbital variability during the Holocene. *Nature Geoscience* **9**: 168-173. DOI: https://doi.org/10.1038/ngeo2608

Erfani E, Mitchell D. 2014. A partial mechanistic understanding of the North American monsoon. *Journal of Geophysical Research* **119**: 13096-13115. DOI: https://doi.org/10.1002/2014JD022038

Estrada AE, SpellenbergR, Lebgue T. 1997. Flora vascular de la laguna de Babicora, Chihuahua, México. *SIDA, Contributions to Botany* **17**: 809-827. DOI: https://www.jstor.org/stable/41967280

Galaz-Samaniego CA, Peñalba MC, Paz-Moreno FA, Espinoza-Encinas IR, Flores-Castro K, Monreal R, Lizárraga-Celaya C. 2023. Lateglacial and Holocene palaeoenvironments at Sierra La Madera, northwestern Mexico: Sharp signals of Younger Dryas and North American monsoon. *Journal of Quaternary Science* **38**: 76-91. DOI: https://doi.org/10.1002/jqs.3464

García-Martínez IM, Bollasina MA. 2020. Sub-monthly evolution of the Caribbean Low-Level Jet and its relationship with regional precipitation and atmospheric circulation. *Climate Dynamics* **54**: 4423-4440. DOI: https://doi.org/10.1007/s00382-020-05237-y

Guzmán-Vázquez I, León-Cruz JF, Galicia L. 2023. Role of dispersal in the altitudinal migration of *Pinus hartwegii* and *Abies religiosa* in mountain systems. *Frontiers in Ecology and Evolution* **11**. DOI: https://doi.org/10.3389/fevo.2023.1150137

Haslett J, Parnell AC. 2008. A simple monotone process with application to radiocarbon-dated depth chronologies. *Journal of the Royal Statistical Society: Series C (Applied Statistics)* **57**: 399-418. DOI: https://doi.org/10.1111/j.1467-9876.2008.00623.x

Haug GH, Hughen KA, Sigman DM, Peterson LC, Röhl U. 2001. Southward migration of the intertropical convergence zone through the Holocene. *Science* **293**: 1304-1308. DOI: https://doi.org/10.1126/science.1059725

Henry LG, McManus JF, Curry, WB, Roberts NL, Piotrowski A M, Keigwin LD. 2016. North Atlantic Ocean circulation and abrupt climate change during the last glaciation. *Science* **353**: 470-474. DOI: https://doi.org/10.1126/science.aaf5529

Hommel G. 1988. A stagewise rejective multiple test procedure based on a modified Bonferroni test. *Biometrika* **75**: 383-386. DOI: https://doi.org/10.1093/biomet/75.2.383

Hutchinson GE, Patrick R, Deevey ES. 1956. Sediments of lake Patzcuaro, Michoacan, Mexico. *Bulletin of the Geological Society of America* **67**: 1491-1504. DOI: https://doi.org/10.1130/0016-7606(1956)67[1491:SOLPMM]2.0.CO;2

Israde-Alcántara I, Velázquez-Durán R, Lozano-García S, Bischoff J, Domínguez Vázquez G, Garduño-Monroy V. 2010. Evolución paleolimnológica del Lago Cuitzeo, Michoacán durante el Pleistoceno-Holoceno. *Boletín de La Sociedad Geológica Mexicana* **62**: 345-357. DOI: https://doi.org/10.18268/BSGM2010v62n3a3

Jackson ST, Overpeck JT. 2000. Responses of plant populations and communities to environmental changes of the late Quaternary. *Paleobiology* **26**: 194-220. DOI: https://doi.org/10.1017/S0094837300026932

Keil P, Mauritsen T, Jungclaus J, Hedemann C, Olonscheck D, Ghosh R. 2020. Multiple drivers of the North Atlantic warming hole. *Nature Climate Change* **10**: 667-671. DOI: https://doi.org/10.1038/s41558-020-0819-8

Koutavas A, Joanides S. 2012. El Niño-Southern oscillation extrema in the Holocene and Last Glacial Maximum. *Paleoceanography* **27**: PA4208. DOI: https://doi.org/10.1029/2012PA002378

Lachniet MS, Vázquez-Selem L. 2005. Last Glacial maximum equilibrium line altitudes in the circum-Caribbean (Mexico, Guatemala, Costa Rica, Colombia, and Venezuela). *Quaternary International* **138-139**: 129-144. DOI: https://doi.org/10.1016/j.quaint.2005.02.010

Leyden BW, Brenner M, Hodell DA, Curtis JH. 1993. Late Pleistocene vlimate in the Central American lowlands. *In:* Swart PK, Lohmann KC, McKenzie J, Savin S, eds. *Climate Change in Continental Isotopic Records*. American Geophysical Union. DOI: https://doi.org/10.1029/GM078

Leyden BW, Brenner M, Hodell DA, Curtis JH. 1994. Orbital and internal forcing of climate on the Yucatan Peninsula for the past ca. 36 ka. *Palaeogeography, Palaeoclimatology, Palaeoecology* **109**: 193-210. DOI: https://doi.org/10.1016/0031-0182(94)90176-7

Lisiecki LE, Raymo ME. 2005. A Pliocene-Pleistocene stack of 57 globally distributed benthic δ 18O records. *Paleoceanography* **20**: PA1003. DOI: https://doi.org/10.1029/2004PA001071

Liu Z. 2023. Evolution of Atlantic meridional overturning circulation since the last glaciation: Model simulations and relevance to present and future. *Philosophical Transactions of the Royal Society A: Mathematical, Physical and Engineering Sciences* **381**: 20220190. DOI: https://doi.org/10.1098/rsta.2022.0190

Lozano-García S, Ortega-Guerrero B. 1994. Palynological and magnetic susceptibility records of Lake Chalco, central Mexico. *Palaeogeography, Palaeoclimatology, Palaeoecology* **109**: 177-191. DOI: https://doi.org/10.1016/0031-0182(94)90175-9

Lozano-García S, Ortega-Guerrero B. 1998. Late quaternary environmental changes of the central part of the Basin of Mexico; correlation between Texcoco and Chalco basins. *Review of Palaeobotany and Palynology* **99**: 77-93. DOI: https://doi.org/10.1016/S0034-6667(97)00046-8

Lozano-García S, Vázquez-Selem L. 2005. A high-elevation Holocene pollen record from Iztaccihuatl volcano, central Mexico. *The Holocene* **15**: 329-338. DOI : https://doi.org/10.1191/0959683605hl814rp

Lozano-García S, Ortega B, Roy, PD, Beramendi-Orosco L, Caballero M. 2015. Climatic variability in the northern sector of the American tropics since the latest MIS 3. *Quaternary Research* **84**: 262-271. DOI: https://doi.org/10.1016/j.yqres.2015.07.002

Lozano-García S, Ortega-Guerrero B, Caballero-Miranda M, Urrutia-Fucagauchi J. 1993. Late Pleistocene and Holocene paleoenvironments of Chalco lake, Central Mexico. *Quaternary Research* **40**: 332-334. DOI: https://doi.org/10.1006/qres.1993.1086

Lozano-García MS, Ortega-Guerrero B, Sosa-Nájera S. 2002. Mid- to Late-Wisconsin pollen record of San Felipe Basin, Baja California. *Quaternary Research* **58**: 84-92. DOI: https://doi.org/10.1006/qres.2002.2361

Lozano-García S, Sosa-Nájera S, Sugiura Y, Caballero M. 2005. 23,000 yr of vegetation history of the Upper Lerma, a tropical high-altitude basin in Central Mexico. *Quaternary Research* **64**: 70-82. DOI: https://doi.org/10.1016/j.yqres.2005.02.010

Lozano-García S, Torres-Rodríguez E, Figueroa-Rangel B, Caballero M, Sosa-Nájera S, Ortega-Guerrero B, Acosta-Noriega C. 2022. Vegetation history of a Mexican Neotropical basin from the late MIS 6 to early MIS 3: The pollen record of Lake Chalco. *Quaternary Science Reviews* **297**: 107830. DOI: https://doi.org/10.1016/j.quascirev.2022.107830

Lozano-García S, Torres-Rodríguez E, Ortega B, Vázquez G, Caballero M. 2013. Ecosystem responses to climate and disturbances in western central Mexico during the late Pleistocene and Holocene. *Palaeogeography, Palaeoclimatology, Palaeoecology* **370**: 184-195. DOI: https://doi.org/10.1016/j.palaeo.2012.12.006

Luo H, Adames ÁF, Rood RB. 2021. A northern hemispheric wave train associated with interannual variations in the Bermuda high during boreal summer. *Journal of Climate* **34**: 6163-6173. DOI: https://doi.org/10.1175/JCLI-D-20-0608.1

Lyle M, Heusser L, Ravelo C, Andreasen D, Olivarez Lyle A, Diffenbaugh, N. 2010. Pleistocene water cycle and eastern boundary current processes along the California continental margin. *Paleoceanography* **25**: PA4211. DOI: https://doi.org/10.1029/2009PA001836

Lynch-Stieglitz J, Schmidt MW, Gene Henry L, Curry WB, Skinner LC, Mulitza S, Zhang R, Chang P. 2014. Muted change in Atlantic overturning circulation over some glacial-aged Heinrich events. *Nature Geoscience* **7**: 144-150. DOI: https://doi.org/10.1038/ngeo2045

Magaña V, Amador JA, Medina S. 1999. The mid-summer drought over Mexico and Central America. *American Meteorologycal Society* **12**: 1577-1588. DOI: https://doi.org/10.1175/1520-0442(1999)012<1577:TMDOMA>2.0.CO;2

Maldonado T, Rutgersson A, Caballero R, Pausata FSR, Alfaro E, Amador J. 2017. The role of the meridional sea surface temperature gradient in controlling the caribbean low-level jet. *Journal of Geophysical Research* **122**: 5903-5916. DOI: https://doi.org/10.1002/2016JD026025

Maloney ED, Hartmann DL. 2000. Modulation of hurricane activity in the gulf of Mexico by the Madden-Julian oscillation. *Science* **287**: 2002-2004. DOI: https://doi.org/10.1126/science.287.5460.2002

Mastretta-Yanes A, Moreno-Letelier A, Piñero D, Jorgensen TH, Emerson BC. 2015. Biodiversity in the Mexican highlands and the interaction of geology, geography and climate within the Trans-Mexican Volcanic Belt. *Journal of Biogeography* **42**: 1586-1600. DOI: https://doi.org/10.1111/jbi.12546

Maza-Villalobos S, Macedo-Santana F, Rodríguez-Velázquez J, Oyama K, Martínez-Ramos M. 2014. Variación de la estructura y composición de comunidades de árboles y arbustos entre tipos de vegetación en la Cuenca de Cuitzeo, Michoacán. *Botanical Sciences* **92**: 243-258. DOI: https://doi.org/10.17129/botsci.104

Metcalfe SE, Barron JA, Davies SJ. 2015. The Holocene history of the North American Monsoon: "known knowns" and "known unknowns" in understanding its spatial and temporal complexity. *Quaternary Science Reviews* **120**: 1-27. DOI: https://doi.org/10.1016/j.quascirev.2015.04.004

Metcalfe SE, O'hara SL, Caballero M, Davies SJ. 2000. Records of Late Pleistocene-Holocene climatic change in Mexico - a review. *Quaternary Science Reviews* **19**: 699-721. DOI: https://doi.org/10.1016/S0277-3791(99)00022-0

Metcalfe S, Say A, Black S, McCulloch R, O'Hara S. 2002. Wet conditions during the last glaciation in the Chihuahuan Desert, Alta Babicora Basin, Mexico. *Quaternary Research* **57**: 91-101. DOI: https://doi.org/10.1006/qres.2001.2292

Moctezuma V, Halffter G, Escobar F. 2016. Response of copronecrophagous beetle communities to habitat disturbance in two mountains of the Mexican Transition Zone: influence of historical and ecological factors. *Journal of Insect Conservation* **20**: 945-956. DOI: https://doi.org/10.1007/s10841-016-9923-5

Muñoz E, Busalacchi AJ, Nigam S, Ruiz-Barradas A. 2008. Winter and summer structure of the Caribbean low-level jet. *Journal of Climate* **21**: 1260-1276. DOI: https://doi.org/10.1175/2007JCLI1855.1

Oka A, Abe-Ouchi A, Sherriff-Tadano S, Yokoyama Y, Kawamura K, Hasumi H. 2021. Glacial mode shift of the Atlantic meridional overturning circulation by warming over the Southern Ocean. *Communications Earth and Environment* **2**: 169. DOI: https://doi.org/10.1038/s43247-021-00226-3

Ortega-Rosas CI, Peñalba MC, Guiot J. 2008. Holocene altitudinal shifts in vegetation belts and environmental changes in the Sierra Madre Occidental, Northwestern Mexico, based on modern and fossil pollen data. *Review of Palaeobotany and Palynology* **151**: 1-20. DOI: https://doi.org/10.1016/j.revpalbo.2008.01.008

Ortega-Rosas CI, Peñalba MC, Guiot J. 2016. The Lateglacial interstadial at the southeastern limit of the Sonoran Desert, Mexico: vegetation and climate reconstruction based on pollen sequences from Ciénega San Marcial and comparison with the subrecent record. *Boreas* **45**: 773-789. DOI: https://doi.org/10.1111/bor.12188

Passalacqua GA, Sheinbaum J, Martinez JA. 2016. Sea surface temperature influence on a winter cold front position and propagation: Air-sea interactions of the "Nortes" winds in the Gulf of Mexico. *Atmospheric Science Letters* **17**: 302-307. DOI: https://doi.org/10.1002/asl.655

Piacsek P, Bernal J.P, Aliaga-Campuzano MP, Chavero LB, Lases-Hernández F, da Cruz FW, Strikís NM, Corona-Martinez L, Ramirez VM, Shimizu MH, Rojas H. 2024. Hydroclimate modulation of central-eastern Mexico by the North Atlantic subtropical high since the little ice age. *Quaternary Science Reviews* **344**: 108981. DOI: https://doi.org/10.1016/j.quascirev.2024.108981

R Core Team. 2024. R: A Language and Environment for Statistical Computing. R Foundation for Statistical Computing, Vienna, Austria. https://www.R-project.org/

Ramírez-Barahona S, Cuervo-Robayo ÁP, Feeley KJ, Ortiz-Rodríguez AE, Vásquez-Aguilar AA, Ornelas JF, Rodríguez-Correa, H. 2025. Upslope plant species shifts in Mesoamerican cloud forests driven by climate and land use change. *Science* **387**: 1058-1063. DOI: https://doi.org/10.1126/science.adn2559

Ritz SP, Stocker TF, Grimalt JO, Menviel L, Timmermann A. 2013. Estimated strength of the Atlantic overturning circulation during the last deglaciation. *Nature Geoscience* **6**: 208-212. DOI: https://doi.org/10.1038/ngeo1723

Rodríguez-Pérez ET. 2018. *Dinámica de la vegetación de la subcuenca de Sayula entre los 51,000 y 6,000 años cal. AP*. MSc Thesis. Universidad Nacional Autónoma de México.

Routson CC, Erb MP, McKay NP. 2022. High latitude modulation of the Holocene North American monsoon. *Geophysical Research Letters* **49**: e2022GL099772. DOI: https://doi.org/10.1029/2022GL099772

Routson CC, McKay NP, Kaufman DS, Erb MP, Goosse H, Shuman BN, Rodysill JR, Ault T. 2019. Mid-latitude net precipitation decreased with Arctic warming during the Holocene. *Nature* **568**: 83-87. DOI: https://doi.org/10.1038/s41586-019-1060-3

Roy PD, Quiroz-Jiménez JD, Pérez-Cruz LL, Lozano-García S, Metcalfe SE, Lozano-Santacruz R, López-Balbiaux N, Sánchez-Zavala JL, Romero FM. 2013. Late Quaternary paleohydrological conditions in the drylands of northern Mexico: A summer precipitation proxy record of the last 80 cal ka BP. *Quaternary Science Reviews* **78**: 342-354. DOI: https://doi.org/10.1016/j.quascirev.2012.11.020

Samuel S, Mathew N, Sathiyamoorthy V. 2023. Characterization of intertropical convergence zone using SAPHIR/Megha-Tropiques satellite brightness temperature data. *Climate Dynamics* **60**: 3765-3783. DOI: https://doi.org/10.1007/s00382-022-06549-x

Salonen JS, Helmens KF, Brendryen J, Kuosmanen N, Väliranta M, Goring S, Korpela M, Kylander M, Philip A, Plikk A, Renssen H, Luoto M. 2018. Abrupt high-latitude climate events and decoupled seasonal trends during the Eemian. *Nature Communications* **9**: 2851. DOI: https://doi.org/10.1038/s41467-018-05314-1

Schiferl J, Kingston M, Åkesson CM, Valencia BG, Rozas-Davila A, McGee D, Wood, A, Chen CY, Hatfield RG,

Rodbell DT, Abbott MB, Bush MB. 2023. A neotropical perspective on the uniqueness of the Holocene among interglacials. *Nature Communications* **14**: 7404. DOI: https://doi.org/10.1038/s41467-023-43231-0

Schneider T, Bischoff T, Haug G. H. 2014. Migrations and dynamics of the intertropical convergence zone. *Nature* **513**: 45-53. DOI: https://doi.org/10.1038/nature13636

Sears PB. 1952. Palynology in southern North America. I: Archeological horizons in the basins of Mexico. *Bulletin of the Geological Society of America* **63**: 241-254. DOI: https://doi.org/10.1130/0016-7606(1952)63[241:PISNAI]2.0.CO;2

Sears PB, Clisby KH. 1955. Palynology in southern North America, part iv: Pleistocene climate in Mexico. *Bulletin of the Geological Society of America* **66**: 521-530. DOI: https://doi.org/10.1130/0016-7606(1955)66[521:PISNA]2.0.CO;2

Stott L, Poulsen C. Lund S. Thunell R. 2002. Super ENSO and global climate oscillations at millennial time scales. *Science* **297**: 222-226. DOI: https://doi.org/10.1126/science.1071627

Straka H, Ohngemach D. 1989. Late Quaternary vegetation history of Mexican highland. *Plant Systematics and Evolution* **162**: 115-132. DOI: https://doi.org/10.1007/BF00936914

Studholme J, Fedorov AV, Gulev SK, Emanuel K, Hodges K. 2022. Poleward expansion of tropical cyclone latitudes in warming climates. *Nature Geoscience* **15**: 14-28. DOI: https://doi.org/10.1038/s41561-021-00859-1

Stuecker MF. 2018. Revisiting the Pacific Meridional Mode. *Scientific Reports* **8**: 3216. DOI: https://doi.org/10.1038/s41598-018-21537-0

Tian Z, Li T, Jiang D, Chen L. 2017. Causes of ENSO weakening during the mid-Holocene. *Journal of Climate* **30**: 7049-7070. DOI: https://doi.org/10.1175/JCLI-D-16-0899.1

Torres-Rodríguez E, Lozano-García S, Figueroa-Rangel BL, Ortega-Guerrero B, Vázquez-Castro G. 2012. Cambio ambiental y respuestas de la vegetación de los últimos 17000 años en el centro de México: El registro del lago de Zirahuén. *Revista Mexicana de Ciencias Geológicas* **29**: 764-778.

Vázquez-Selem L, Heine K. 2011. Chapter 61 - Late Quaternary Glaciation in Mexico. *Developments in Quaternary Science* **15**: 849-861. DOI: https://doi.org/10.1016/B978-0-444-53447-7.00061-1

Viechtbauer W. 2010. Conducting meta-analyses in R with the metafor package. *Journal of Statistical Software* **36**: 1-48. DOI: https://doi.org/10.18637/jss.v036.i03

Waliser DE, Jiang X. 2015. Tropical meteorology and climate: Intertropical convergence zone. *Encyclopedia of Atmospheric Sciences: Second Edition, Vol. 6*. Elsevier. DOI: https://doi.org/10.1016/B978-0-12-382225-3.00417-5

Wang C. 2007. Variability of the Caribbean Low-Level Jet and its relations to climate. *Climate Dynamics* **29**: 411-422. DOI: https://doi.org/10.1007/s00382-007-0243-z

Wang C, Lee SK. 2007. Atlantic warm pool, Caribbean low-level jet, and their potential impact on Atlantic hurricanes. *Geophysical Research Letters* **34**: L02703. DOI: https://doi.org/10.1029/2006GL028579

Wang H, Zuo Z, Zhang K, Bu L, Xiao D. 2023. Evolution characteristics of the Atlantic meridional overturning circulation and its thermodynamic and dynamic effects on surface air temperature in the Northern Hemisphere. *Science China Earth Sciences* **66**: 1185-1211. DOI: https://doi.org/10.1007/s11430-022-1102-y

Watts WA, Bradbury JP. 1982. Paleoecological Studies at Lake Patzcuaro on the West-Central Mexican Plateau and at Chalco in the Basin of Mexico. *Quaternary Research* **17**: 56-70. DOI: https://doi.org/10.1016/0033-5894(82)90045-X

Whittaker RH, Levin SA, Root RB. 1973. Niche, Habitat, and Ecotope. *The American Naturalist* **107**: 321-338.

Williams JW, Jackson ST. 2007. Novel climates, no-analog communities, and ecological surprises. *Frontiers in Ecology and the Environment* **5**: 475-482. DOI: https://doi.org/10.1890/070037

Xelhuantzi-López MS. 1991. *Estudio palinológico y reconstrucción paleoambiental del ex-lago de Zacapu, Michoacán*. MSc Thesis. Universidad Nacional Autónoma de México.

Yuan S, Chiang HW, Liu,G, Bijaksana,S, He S, Jiang X, Imran AM, Wicaksono SA, Wang X. 2023. The strength,

position, and width changes of the intertropical convergence zone since the Last Glacial Maximum. *Proceedings of the National Academy of Sciences of the United States of America* **120**: e2217064120. DOI: https://doi.org/10.1073/pnas.2217064120

Zhang R, Delworth T. 2005. Simulated tropical response to a substantial weakening of the Atlantic. *Journal of Climate* **18**: 1853-1860. DOI: https://doi.org/10.1175/JCLI3460.1

Associate editor: Arturo de Nova

Supporting agencies: This study was funded by DGAPA-PAPIIT IN105324. Manuel Zepeda Pirron is a doctoral student from the Posgrado en Ciencias de la Tierra, Universidad Nacional Autónoma de México (UNAM) and has received SECIHTI fellowship (CVU 1085983).

Author contributions: MZP, writing analysis, conceptualization, designed the review and the meta-analysis, SLG, designed and directed the review, MC, conceptual review, KO, conceptual review. The authors declare that there is no conflict of interest, financial or personal, in the information, presentation of data and results of this article.